A Scale Model Study of Displacement Ventilation with Chilled Ceilings

by

Katherine J.A. Holden

M.A. Hons. Engineering,
Cambridge University, England, 1989

Submitted to the Department of Architecture
in partial fulfillment of the requirements for the degree of

Master of Science
in Building Technology

at the

Massachusetts Institute of Technology
June 1995

Signature of Author .....
Katherine J.A. Holden
Department of Architecture
May 12th, 1995

Certified by .....

Leslie K. Norford
Associate Professor
of Building Technology
Thesis Co-supervisor

Leon R. Glicksman
Professor of Building Technology
and Mechanical Engineering
Thesis Co-supervisor

Accepted by .....
Leon R. Glicksman
Chair, Departmental Committee on Graduate Students

A Scale Model Study of
Displacement Ventilation with Chilled Ceilings

by

Katherine J.A. Holden

Submitted to the Department of Architecture on May 15th, 1995
in partial fulfillment of the requirements for the degree of
Master of Science in Building Technology

Abstract

Displacement ventilation is a form of air-conditioning which provides good air quality and some energy savings. The air quality is better than for a conventional mixed ventilation system. The maximum amount of cooling that displacement ventilation can provide whilst maintaining a comfortable space is between 25 and 40 W/m^2. Chilled ceilings can be added to increase the cooling capacity of the system. A scale model study was carried out to determine comfort levels at different conditions, to establish maximum cooling loads and to observe flow patterns in a typical office room with displacement ventilation and a chilled ceiling. Refrigerant R114 was used as the scaling fluid and an existing test box was used as the model room. Heat sources were simulated using electric resistances in aluminum enclosures. A gas and a water circuit were built to supply ventilation and cooling to the room. Flow visualization was carried out by injecting refrigerant laden with ammonium chloride smoke into the supply point. The smoke was lit by a spotlight shone between two pieces of cardboard and images were taken using a video camera.

The results showed that for displacement ventilation alone, the temperature distribution was within stringent comfort levels for heat loads up to 25 W/m^2 with an air change rate of 7.5. When a chilled ceiling was added, up to 40 W/m^2 could be cooled within comfort levels. The refrigerant was radiatively absorbing, so the radiation cooling from the ceiling was reduced. Therefore, this maximum cooling load is probably an underestimate. Some displacement occurred at low levels for this cooling load, which indicated good air quality, but it was below the breathing zone. At higher loads, the flow appeared to be mixed. Therefore, the benefit of enhanced air quality with displacement ventilation was lost when a chilled ceiling was added.

The use of a scale model allowed the study of ventilation systems without building a full scale room. It was of limited use for this study because the heat transfer by radiation could not be modelled correctly with this refrigerant. Further experiments could be carried out with lower supply air rates. The experiments could be improved by ensuring more accurate measurement of the water and gas flow rates and temperatures, reducing heat losses. Flow visualization could be improved by injecting smoke at different points within the room and by using a stronger, more focused plane of light. The apparatus could be used for future work on heat transfer that does not involve a significant amount of radiation. It is recommended that a more leak-tight box with a greater height is built and a more environmentally friendly refrigerant is used.

Thesis supervisors:	Leon R. Glicksman	Leslie K. Norford
Titles:	Professor of Building Technology and Mechanical Engineering	Associate Professor of Building Technology

Acknowledgements

I would like to thank Professors Glicksman and Norford for their help and advice, both theoretical and practical.

Sponsorship for this degree was given by the Engineering and Physical Sciences Research Council. Thanks to Ove Arup & Partners for the Peter Dunican Award and for giving me leave of absence.

Frenger of Alberta, Canada provided considerable assistance by donating a radiant panel, as did Andy Phahnl with help writing the data acquisition software.

I am enormously grateful to Mehmet Okutan, who helped design and build the apparatus with me for his own research. His hard work and organization made it possible to finish the project in time and his good company made it enjoyable. Thanks also to Annie Liu and Peter Cho for their assistance.

Thanks to Mark DeSimone for invaluable advice on the design of plumbing systems and how to glue PVC and solder copper. Thanks to all the Building Technology students for keeping me amused and for putting up with the terrible smells and noise from our work space.

I thank my family, Mum, Bob, Dad, Anni, Angie and Alice, for their support and encouragement over the years.

I also thank Rose and Diana for great friendship and happy times.

Table of contents

List of figures and tables

Figures

Tables

1. Introduction

1.1 Displacement ventilation

Displacement ventilation has been used in Europe, and particularly Scandinavia, for many years. It is a type of air-conditioning which provides good air quality and some energy savings. Air is supplied at low level at a just below room temperature and spreads out across the floor. When it reaches a heat source such as a person or a computer, it rises in a buoyant plume, taking contaminants from the heat source with it. The hot air forms a stratified layer below the ceiling, where it is extracted. Displacement ventilation works well in spaces with high ceilings, such as in industrial applications or public halls, but it has some limitations when used in offices. It creates a temperature gradient in the occupied space. To maintain a comfortable space, according to International Standard ISO 7730[1], the air temperature difference should be no greater than 3K between 0.1 m and 1.1 m above the floor, i.e. ankle to head height for someone sitting down. ASHRAE Standard 55-1981[2] stipulates no more than 3 K between 0.1 and 1.7 m, which is a considerably more stringent standard. These standards are supported by laboratory research by Olesen, Scholer and Fanger[3], who predicted 5% dissatisfied with a 2.8 K difference between 0.1 and 1.1 m and 10% dissatisfied with 3.7 K. Also there is a risk of draft from the cool supply air, particularly round the ankles, as there can be significant draft near the supply diffuser. Fishman and Semere[4] and Fishman and Underwood[5] studied cold air currents along the floor of a 23°C room; 24°C was preferred for ideal foot comfort, but even 19°C corresponded to "comfortably cool" on average, with only about 20% dissatisfied. Air velocities below 0.25 m/s were found to have little influence on foot comfort in these experiments. These two comfort criteria dictate that the maximum amount of cooling that can be provided in an office space is 40 W/m^2. However, the heat loads in offices are often greater than 40 W/m^2.

1.2 Cooled ceilings

It has been suggested that the amount of cooling provided by a displacement ventilation system can be increased by combining it with a cooled ceiling. Cooled ceilings have been used in Europe for at least twelve years, although they are relatively rare in North America. Cooled water is run through a closed circuit which is thermally connected to metal panels. The temperature of these panels is lowered below the room temperature and cooling occurs by radiation and convection. The amount of heat transfer by radiation can be up to 55%. A cooled ceiling only removes the sensible heat from the space, not the latent load. The latent load must be removed by a separate ventilation system, which also provides outside air. The supply air may have to be dehumidified, to control humidity levels in the space and to keep the dewpoint below the lowest surface temperature of the ceiling, to avoid condensation forming. The panels can be integrated with a conventional modular suspended ceiling and they typically cover 50% of the ceiling. They can provide at least 150 W/m^2 of cooling.

1.3 Aims

Whilst the combination of displacement ventilation and a cooled ceiling seems attractive for cooling loads of over 40 W/m^2, not much is known about the interaction of the two systems, in terms of comfort and air quality. A scale model will be used to investigate temperature gradients, comfort levels and flow patterns for an air-conditioning system in an

office which combines displacement ventilation and a cooled ceiling. Maximum heat loads will be evaluated that maintain comfortable temperature distributions for different supply air rates. Displacement ventilation works on the principle of supplying cool air at low level which rises up around the heat sources. The convective part of cooling from a cooled ceiling cools the air nearest the ceiling and could counteract the buoyant flows or form a separate circulation pattern. The proportions of cooling by displacement ventilation and the cooled ceiling will be varied to see what conditions must apply to keep improved air quality associated with displacement ventilation. Flow visualization will be used to observe the flow patterns of the combined systems at different conditions. The reliability of the scale model for investigating flow patterns and temperature distributions within an enclosed space will be analyzed. Recommendations for future work associated with displacement ventilation and cooled ceiling will be made, as well as suggestions for modifications to the scale model.

1.4 Scale model

A physical model was used for the study, which had been built and proven by Olsen[4]. It consisted of a box with walls made of aluminum panels and insulation and a floor and ceiling of plexiglass, supported by a dexion frame. It had electric resistance heaters in all four walls and tubing for supplying cooled water to three of the walls. It was chosen because it was available, it could be used in a laboratory and it could be easily modified to simulate a variety of designs and thermal conditions. The facilities and funds were not available to use a full scale model.

1.5 Overview of thesis

This thesis describes the current knowledge about displacement ventilation and cooled ceilings as well as scale model studies and flow visualization. The scaling method used involves matching the relevant non-dimensional parameters for natural convection, which were Grashof number, Prandtl number and Reynolds number. The radiation heat transfer was not accurately scaled. A suitable scaling fluid was searched for and a dense gas, refrigerant R114 was chosen. Its properties are given, as well as those of the other gases, and the properties of mixtures of R114 with small amounts of air are calculated. The existing model is described and so is the design of the additions and modification to the model inside, the external gas circuit for supplying the gas to the box, the water circuit for cooling the gas and the cooled ceiling water circuit. Flow and temperature measurements are described, including calibration of thermocouples and the heat exchanger. The use of refrigerant is outlined. Uncertainty levels are estimated and they indicate the reliability of the results.

The experiments consist of one set with displacement ventilation alone with varying heat loads and another set with a cooled ceiling added. The supply rate of the fluid was kept constant and the heat loads and amount of cooling by the cooled ceiling were varied, to investigate how the temperature gradients and flow patterns varied as the proportion of cooling done by the two systems varied. This was repeated for a larger supply rate of fluid.

2. Literature review

2.1 Displacement ventilation

There have been several experimental and analytical studies of displacement ventilation, mainly in Europe. A good overview is provided by A.G.L. Svensson[7]. Svensson discusses the current state of displacement systems with regard to air exchange efficiency, ventilation efficiency and thermal comfort and compares the advantages and disadvantages of displacement systems and mixing systems. Heat loads of about 30 W/m^2 can be removed at normal room heights (2.7 - 2.8 m) with no loss of comfort and with an air quality superior to that of mixing ventilation. For normal comfort levels, the temperature difference between the elevations of 1.8 m and 0.1 m above the floor must not exceed 2 to 3 K. With room heights of about 3.4 m, heat loads of some 40 W/m^2 can be removed. For larger heat loads, it had become common to combine displacement ventilation with cooled ceilings. The combination with a radiation type of cooled ceiling could then cool a maximum of 70 W/m^2. For loads greater than 40 W/m^2 with displacement ventilation alone, the temperature gradients in the occupied zone become too large for comfort, so Svensson recommended that third generation devices with special ejector parts be used to supply air in such a way that room air from the occupied zone is co-ejected with the primary air, to provide mixing in the occupied zone, called the low-velocity technique.

Sandberg and Blomqvist[8] describe laboratory tests to determine if displacement ventilation gave rise to better air quality in office rooms than with a mixing system. Air quality is quantified using the room average ventilation effectiveness which is the equilibrium concentration of pollutants in the extract duct divided by the room average concentration. The other useful quantity is air exchange effectiveness which is the ratio between the turnover time for the ventilation air and the turnover time for the air in the room. They found that large flow rates were needed to attain better air quality in the occupied zone than if the room were ventilated by a mixing system. Otherwise, the stratified layer where the hot, polluted air gathers before it is exhausted starts below the breathing zone. The temperature and concentration profiles were not alike. To avoid uncomfortable drafts, supply air terminals that spread the air over a large sector must be used.

Seppänen, Fisk, Eto and Grimsrud[9] compared conventional mixing and displacement ventilation systems in US commercial buildings in different climates. Energy consumption and indoor environmental conditions were evaluated using a computer simulation, and first costs were estimated based on published unit cost data and information provided by manufacturers. Data on the air temperature and pollutant concentration were taken from laboratory measurements and used as inputs to the programs. They found that displacement ventilation seemed to create much better average air quality in the occupied zone than traditional mixing VAV systems with recirculation. Displacement ventilation did not have much influence on energy consumption, however, its first cost is significantly increased due to required cooling panels if the cooling load exceeds 40 W/m^2.

Mattson and Sandberg[10] investigated the influence of physical activity on the performance of displacement ventilation. They simulated a human walking back and forth at a slow velocity in an office, using a thermal manikin in a full scale test room. Both air exchange efficiency and ventilation efficiency became higher when the dummy moved slowly compared to when it was at rest, with an optimum velocity of about 0.3 m/s. One possible explanation was that some of the naturally convected air along the dummy was swept away and settled in the surrounding air, instead of directly rising towards the ceiling by the

plume, which tends to cause some macro air circulation in the upper part of the room. In this way, the main air flow pattern of the room could become more unidirectional - from the bottom of the room towards the top - which would increase the efficiency values. There could also be a "cleaning up" effect in the locked in area, swept by the dummy plume. At higher velocities, the efficiencies decreased and approached the values of a mixed system. This was probably due to increased vertical turbulence near the dummy, especially around its "head". A stronger temperature gradient in the room caused better efficiency and less sensitivity to manikin movements.

2.2 Cooled ceiling

The only investigation of thermal comfort in rooms with cooled ceilings and displacement ventilation that this author knows of is by Kulpmann[11]. He ran experiments in a full scale test room and evaluated thermal comfort and air quality. With the cooled ceiling alone, the increase in air temperature in the room was practically negligible. The room surface temperatures were about the same as the air temperatures and the floor temperature was slightly lower, due to the intense radiation exchange with the cooled ceiling surface. The tests were for cooling loads of between 35 and 101 W/m^2. When the displacement ventilation system was added there was a temperature difference in the lower part of the room. The temperature increase from a height of 0.1 m to 1.1 m amounted to 1.5 K for a cooling load of 52 W/m^2, an air change rate per hour of 3.2 and a supply velocity of 0.27 m/s. The ventilation contributed 25% of the cooling capacity. The air quality was much better than for a mixing system at low heights when displacement ventilation contributed at least 25% of the cooling. However, at the breathing zone for a person sitting down, 1.1m, the air quality was only better for one case. The cooling by the ventilation contributed 36%, the total cooling load was 25 W/m^2 and the air change rate per hour was 3.2. For the other displacement ventilation cases, the air became close to fully mixed above 0.6 m, which is below the breathing zone, and with the cooled ceiling alone, the air seemed to be fully mixed.

3. Scaling

3.1 Theory

The aim of building the scale model of a room is to study the temperature distributions and fluid flows that occur in a room, without having to build a full scale room. This is done by using dimensional analysis. The governing equations are non-dimensionalized by dividing the variables by characteristic constants or combinations of constants of the same dimension. Then if all the coefficients of the non-dimensionalized variables are made the same, the model and the prototype will be similar. These coefficients are used to form dimensionless parameters which are commonly used to characterize characterize the thermal and flow properties of a system. Dimensionless analysis allows the experimental data and analysis of results to be conveniently and concisely organized to show the relationships between dimensionless groups of relevant variables. Important properties of the full scale system can then be predicted.

Momentum transfer and convective heat transfer are the main phenomena being studied. Radiation is also significant. The flow is forced in at the diffuser by the fan, but the flows around the model heat sources are buoyant, occurring by natural convection. For steady, laminar, two dimensional, incompressible flow with constant viscosity and negligible viscous dissipation, the relevant equations which govern the flows are:

Mass $$\frac{du}{dx} + \frac{dv}{dz} = 0$$

Momentum in z direction $$\rho u\frac{\partial v}{\partial x} + \rho v\frac{\partial v}{\partial z} = -\frac{\partial P}{\partial z} + \mu\left(\frac{\partial^2 v}{\partial x^2} + \frac{\partial^2 v}{\partial z^2}\right) - \rho g$$

Energy equation $$u\frac{dT}{dx} + v\frac{dT}{dz} = \alpha\left(\frac{\partial^2 T}{\partial x^2} + \frac{\partial^2 T}{\partial z^2}\right)$$

Far from the wall, velocity gradients are zero, and the z momentum equation reduces to

$$-\frac{\partial P}{\partial z} = \rho_e g$$

Substituting back gives

$$\rho u\frac{\partial v}{\partial x} + \rho v\frac{\partial v}{\partial z} = \mu\left(\frac{\partial^2 v}{\partial x^2} + \frac{\partial^2 v}{\partial z^2}\right) + g(\rho_e - \rho)$$

Now assume constant properties except for the density difference in the buoyancy force. Since $\rho = \rho(P,T)$, a Taylor expansion gives

$$\rho_e - \rho = \left(\frac{\partial \rho}{\partial T}\right)_P (T_e - T) + \left(\frac{\partial \rho}{\partial P}\right)_T (P_e - P) + \text{higher order terms}$$

In the boundary layer assume $P \sim P_e$ so

$$\frac{\rho_e - \rho}{\rho} = -\left(\frac{\partial \rho}{\partial T}\right)_P (T - T_e) = \beta(T - T_e)$$

where β is the volumetric coefficient of thermal expansion. For an ideal gas, $\beta = 1/T$.

The resulting z momentum equation is

$$u\frac{\partial v}{\partial x} + v\frac{\partial v}{\partial z} = \nu\left(\frac{\partial^2 v}{\partial x^2} + \frac{\partial^2 v}{\partial z^2}\right) + g\beta(T - T_e)$$

The governing equations are non-dimensionalized using the following dimensionless variables:

Positions $\quad x^* = \frac{x}{L}, \qquad z^* = \frac{z}{h}$

L is the length of the room and h is the height.

Velocity $\quad v^* = \frac{v}{v_b}, \qquad u^* = \frac{u}{(L/h)v_b},$

v_b is the buoyant velocity, found from balancing the inertia and buoyancy forces.

$$\frac{v_b^2}{h} \sim g\beta(T - T_e)$$

$$v_b = \sqrt{g\beta(T - T_e)h}$$

Temperature $\quad \theta^* = \frac{T - T_e}{T_s - T_e}$

These normalized values can be used to compare this study with others and with real displacement ventilation systems. They are the same for the model as for the full scale room. The y position is non-dimensionalized in the same way as the other two dimensions. Also, the aspect ratios characterize the geometry of the room, relating the width, w, and the length, l, to the height, h.

Y position $\quad y^* = \frac{y}{w}$

Aspect ratios $\quad A_w = \frac{h}{w}, \; A_l = \frac{h}{l}$

The scaled governing equations are:

mass $\quad \frac{du^*}{dx^*} + \frac{dv^*}{dz^*} = 0$

momentum $\quad \frac{v_b^2}{h}\left(u^*\frac{\partial v^*}{\partial x^*} + v^*\frac{\partial v^*}{\partial z^*}\right) = \frac{\nu v_b}{L^2}\left(\frac{\partial^2 v^*}{\partial x^{*2}} + \frac{\partial^2 v^*}{\partial z^{*2}}\right) + g\beta(T_s - T_e)\theta^*$

energy $\quad \frac{v_b(T_s - T_e)}{h}\left(u^*\frac{d\theta^*}{dx^*} + v^*\frac{d\theta^*}{dz^*}\right) = \frac{\alpha(T_s - T_e)}{L^2}\left(\frac{\partial^2\theta^*}{\partial x^{*2}} + \frac{\partial^2\theta^*}{\partial z^{*2}}\right)$

For Prandtl number, $Pr = \nu/\alpha \sim 1$, which is the case for air at standard conditions, the viscous forces are comparable in magnitude to the buoyancy force, as well as the inertia force, so:

$$\frac{v_b^2}{h} \sim g\beta(T_s - T_e) \sim \frac{\nu v_b}{L^2}$$

which solves to give

$$\frac{L}{h} \sim \left(\frac{\nu^2}{g\beta(T_s - T_e)h^3}\right)^{1/4} \qquad \text{and } v_s \sim (g\beta(T_s - T_e)h)^{1/2}$$

The dimensionless group is the Grashof number, Gr

$$Gr = \frac{g\beta(T_s - T_e)h^3}{\nu^2} \qquad \text{and } \frac{L}{h} = \frac{1}{Gr^{1/4}}$$

Therefore, the Grashof number should be matched to scale the natural convection characteristics of the system correctly. The Rayleigh number, Ra, equals Gr Pr, so for Pr = 1, the Rayleigh number could be used as an alternative to the Grashof number.

3.2 Length and temperature difference scales

The length scale, h_r, was determined by matching the Grashof number for the full scale room and the model, based on the height of the room, h.

$$\frac{\beta_f \Delta T_f g_f h_f^3}{\nu_f^2} = \frac{\beta_m \Delta T_m g_m h_m^3}{\nu_m^2}$$

Initially, a fluid was required that allowed the temperature difference scale to be kept at unity, to make temperature readings and analysis of data easy. The height of the model was fixed by the dimensions of the existing box, 0.41 m including a false ceiling and floor and a height of 2.7 m was required to simulate a typical full scale room. The corresponding length scale was 6.6. The coefficient of expansion and the kinematic viscosity depended on the properties of the fluid chosen. The kinematic viscosity was the main factor as it depended on density and dynamic viscosity, and the density of the fluid was much greater than that of air. The gravity constant was the same for the full scale room and the model. Therefore:

Length scale

$$\frac{h_f^3}{h_m^3} = \frac{\beta_m}{\beta_f} \cdot \frac{\Delta T_m}{\Delta T_f} \cdot \frac{\nu_f^2}{\nu_m^2}$$

or

$$h_r^3 = \frac{\nu_r^2}{\beta_r \Delta T_r}$$

$$h_r = \left(\frac{\nu_r^2}{\beta_r \Delta T_r}\right)^{1/3}$$

where x_f = full scale value of variable x
x_m = model value of variable x

and $x_r = \frac{x_f}{x_m}$, the ratio of full scale to model values.

For a temperature difference scale of unity,

$$h_r = \left(\frac{\nu_r^2}{\beta_r}\right)^{i/3}$$

However, the best length scale derived from fluids that could be found was 4.6 (See Chapter 4). So, the only remaining variable was the temperature difference scale, which was found by setting the length scale to 6.6.

Temperature difference scale $\Delta T_r = \dfrac{\nu_r^2}{\beta_r h_r^3}$

3.3 Velocity scale

The velocity of the supply air into the room was scaled to maintain similarity of Reynolds number. The Archimedes number was also matched, as it characterized the ratio between the buoyancy and the inertia of the airflow coming from the supply air diffuser, based on the height of the diffuser, H. Assuming that the fluid behaves like an ideal gas, scaling based on Reynolds number, Archimedes number or the buoyant velocity gives the same result. This is found by substituting the length scale from the Grashof number and using the approximation:

$$\beta = \frac{1}{T_a} \quad \text{for an ideal gas.}$$

Reynolds number $Re_H = \dfrac{\rho u_s H}{\mu}$ or $Re_H = \dfrac{u_s H}{\nu}$

Archimedes number $Ar = \dfrac{g\Delta T H}{T_a u_s^2}$ or $\dfrac{\text{buoyant velocity}^2}{\text{initial mean velocity}^2}$

where initial mean velocity, $u_s = \dfrac{q}{A}$

and buoyant velocity, $v_b = \sqrt{g\beta\Delta T H}$

Velocity scale $\dfrac{u_f H_f}{\nu_f} = \dfrac{u_m H_m}{\nu_m}$

or $\dfrac{u_f}{u_m} = \dfrac{H_m}{H_f} \cdot \dfrac{\nu_f}{\nu_m}$

$$u_r = \frac{\nu_r}{H_r}$$

The design condition for the full scale case was an initial mean velocity of supply air of 0.1 m/s for a heat load of 40 W/m^2. The flow rate of the supply air was Q and the free area of the diffuser was A_s. This area was found by looking at manufacturers' catalogues and specifications for low velocity diffusers.

3.4 Volume flow rate scale

The flow rate scale is found by making similarity between the velocity of the supply air at the diffuser and the area of the diffuser for the two cases. The area scales as the square of the length.

Supply air flow rate, $Q = u A_S$

$Q_r = u_r A_{sr}$

$Q_r = u_r h_r^2$

3.5 Mass flow rate scale

Mass flow rate, $m = \rho Q$

$m_r = \rho_r Q_r$

3.6 Power scale

The power scale was related to the cooling required, which was found from the mass flow rate scale and the temperature difference scale. The temperature difference was between the supply air temperature and the extract air temperature. For each heat load case, this temperature difference was kept the same and the flow rate was calculated in order to provide the required cooling. This meant that a higher heat load required a greater supply air velocity. The temperature difference and velocity in the full scale =could be adjusted to optimize the comfort in the space, depending on whether the temperature gradient or the draft at low level were more significant.

$$q = m c_p (T_e - T_s)$$

$$q_r = m_r c_{pr} \Delta T_r$$

3.7 Power intensity scale

The power intensity is found by dividing the heat load by the floor area. It is very useful for characterizing the heat load in a space.

$$q'' = \frac{q}{A}$$

$$q''_r = \frac{q_r}{A_r}$$

$$q''_r = \frac{q_r}{h_r^2}$$

3.8 Radiation

Heat transfer by radiation can be approximated for an enclosure where the surface temperature T_S is nearly equal to the temperature of the rest of the enclosure, T_E. In this study, most of the radiation transfer occurs between the ceiling and the floor, although there is also some from the heated side wall for the higher heat load cases. For transparent fluids,

$$Q_{rad} = \varepsilon_c 4\sigma T_c^3 (T_c - T_e) A_c$$

At a surface i in a room of N small isothermal gray surfaces with equal areas and emissivities of greater than 0.9, the equation for heat balance at steady state is:

$$q_i'' = -k \frac{\partial T}{\partial n} + \sigma\varepsilon T_{si}^4 - \sigma\varepsilon \sum_{j=1}^{N} F_{ij} T_{sj}^4$$

For forced convection with $q'' = \rho c_p u \Delta T$, the non-dimensionalized form is:

$$q_i''^* = - \frac{1}{Pr\ Re} \frac{\partial T^*}{\partial n^*} + \frac{1}{Pl\ Pr\ Re} \sum_{j=1}^{N} F_{ij}^* (T_{si}^* - T_{sj}^*)$$

where Planck number, $Pl = \dfrac{k}{4\sigma T_o^3 H\varepsilon}$ and $Pr\ Re = \dfrac{uH}{\alpha}$

For natural convection with $q'' = h\Delta T$, the non-dimensionalized form is:

$$q_i''^* = - \frac{1}{Nu} \frac{\partial T^*}{\partial n^*} + \frac{1}{Pl\ Nu} \sum_{j=1}^{N} F_{ij}^* (T_{si}^* - T_{sj}^*)$$

where Nusselt number, $Nu = \dfrac{h_c H}{k}$ and h_c = convective heat transfer coefficient.

Pl Nu gives an estimate of the ratio of natural convection to radiation, and Pl Pr Re compares heat transported by ventilation to radiation, so these two combinations of dimensionless parameters should match.

For scaling the radiation interaction, the two fluids should have the same emission and absorptance characteristics. Either they should both be transparent or both opaque, or they should have the same product of mean absorption coefficient, a and characteristic dimension, H, if they can be modelled as gray emitters. The product, aH is the optical depth of enclosure. For a transparent fluid, $aH << 1$ and for an opaque fluid, $aH >> 1$.

4. Scaling Fluid Study

4.1 Important parameters

The scaling fluid was chosen to match the relevant dimensionless numbers for air, as described in the previous section. The first one that was considered was Prandtl number, because this depends on the properties of the fluid at a given temperature and pressure. It was preferred to keep these conditions the same for the prototype and the model. Then the Grashof number was matched. The variables were length and, if necessary, temperature difference. The coefficient of expansion was kept the same, as it mainly depends on absolute temperature for gases, and so was the gravity constant .

This meant that the most suitable fluid was a gas with a high density compared to air. There are several refrigerant gases which have high densities. If the temperature, temperature difference, pressure and gravity constant are kept the same, then for a given fluid, the length scale is determined by the kinematic viscosity. For air at 20°C and 1 atm., its Prandtl number is 0.7 and its kinematic viscosity is 1.51×10^{-5} m^2/s.

4.2 Refrigerant R114

The scaling fluid which was used in Olsøn's small scale study of natural convection was R114, dichlorotetraflouroethane (1,2-dichloro-1,1,2,2-tetrafluoroethane). This refrigerant has an ozone depletion potential (ODP) of 0.8 and a global warming potential (GWP) of 4500. It is not toxic or corrosive and it is inflammable. It has become very expensive, possibly because it is being phased out and its main use is in naval applications. It costs $11.5 /lb or $25.5 /kg, compared with $1 /kg in 1986.

It has a density which is 7 times that of air and a viscosity about 5/8ths that of air and a kinematic viscosity about 1/10th that of air. Its Prandtl number at standard conditions is 0.8. If all other factors are kept constant, the length scale is 4.6. The gas is radiatively absorbing and emitting, and it is not nearly as transparent as air, although it is much less opaque than water.

4.3 Other refrigerants

Other refrigerants were looked for which had similar or better properties and which were less harmful to the environment. From the data given in ASHRAE Fundamentals Handbook 1993, Chapter 17, R134a, R124, R125, R142b, and R152a were potential choices. Their Prandtl numbers matched air quite well, but their kinematic viscosities were generally too low to give significant scaling factors. If the temperature difference were to not be scaled, a length scale of at least 6 would have been required to make a realistic height of an office, using the existing model. The scaling factors for these refrigerants were between 2.6 and 3.9. See Table 4.1.

Some other refrigerants were investigated, which have been developed recently and are not yet commonly sold. They were R218, RC318 and R227ea. The thermal properties were provided by the National Institute of Standards and Technology (NIST), from their program "REFPROP". The Prandtl numbers matched air better, at around 0.76, and the scaling factors were higher, at 4.4 to 5.2. These refrigerants were much less harmful to the

environment, with ODPs of 0.00 and GWPs of around 2000. However, they were all very expensive, at $950 /kg to $2250 /kg. Therefore, R114 was used again. As it is being phased out, its availability is limited.

4.4 Design conditions

Table 4.2 shows the scaling factors for R114 and the full scale and model values of the design conditions for different heat load cases. Table 4.3 shows the scaling factors and change in properties for R114 when it is mixed with some air. Table 4.4 shows how the design conditions are affected by the addition of some air into the refrigerant for a typical case with a heat load of 40 W/m^2.

The absorptance of R114 was estimated using spectral absorptance data measured by Olson[6], given in Appendix A, figure A.1, page 225. The figure shows that there are some strongly absorbing bands, especially between wavelengths of 8 and 17μ. Siegel and Howell[12] list the fraction of radiation emitted by a blackbody up to a given wavelength-temperature product, λT, in Appendix, table A-5, page 739. The surface temperature of the ceiling was approximately 300 K. For this temperature, the blackbody fraction of energy transmitted for dry air was estimated at different wavelengths and the average transmittance for R114 was read for the section between each pair of wavelengths. The blackbody fraction of energy transmitted for R114 was calculated by finding the blackbody fraction for each section by multiplying the average transmittance for that section with the blackbody fraction for dry air and then adding it to the previous fraction, to give a cumulative total. See table 4.5.

Table 4.5 Blackbody fraction of radiation energy transmitted for R114

Wavelength, μm	Wavelength-temperature product, μm K	Blackbody fraction for dry air	Average transmittance of section, τ	Blackbody fraction for R114
4	1200	0.002	1.0	0.002
8	2400	0.14	0.7	0.1
13	3900	0.46	0.0	0.1
17	5400	0.68	0.3	0.17
40	12000	0.94	0.7	0.35
55	16500	0.98	0.4	0.37

Therefore, at temperatures of around 300 K, refrigerant R114 transmits about 37% and absorbs about 63% of the radiation energy from a surface. Olson calculated the mean absorption coefficient to be $a = 0.135\ cm^{-1}$.

The typical length of the enclosure is the height, H = 41 cm. The optical depth can be used to scale the absorptance characteristics of the fluids. For R114, optical depth, aH = 5.5. Dry air is transparent and aH << 1, so the radiation absorptance is not matched well. Other refrigerants would also be radiatively absorbing, so it would be difficult to match this property well.

Table 4.1 Refrigerant properties and scaling factors

Fluid	Symbol	Air	Water	R114	RC318	R227ea	R218
Density (kg/m3)	ρ	1.2	998.2	7.35	8.69	7.3	8.03
Viscosity (kg/m s)	μ	1.82E-05	1.00E-03	1.14E-05	1.10E-05	1.17E-05	1.23E-05
Kinematic viscosity (m^2/s)	ν	1.51E-05	1.00E-06	1.55E-06	1.26E-06	1.61E-06	1.53E-06
Specific heat (J/kg K)	c_p	1005	4183	706.7	796	813	790.9
Conductivity (W/mK)	k	0.0261	0.5984	0.0101	0.0114	0.0126	0.0128
Thermal diffusivity (m^2/s)	α	2.16E-05	1.43E-07	1.94E-06	1.65E-06	2.12E-06	2.02E-06
Prandtl number	Pr	0.701	7.00	0.796	0.767	0.758	0.758
Ambient temp (K)	T	293	293	293	293	293	293
Coeff. thermal exp (/K)	β	3.41E-03	2.27E-04	3.76E-03	3.41E-03	3.41E-03	3.41E-03
Grashof number	Gr	1.16E+10	1.16E+10	1.16E+10	1.16E+10	1.16E+10	1.16E+10
Rayleigh number	Ra	8.07E+09	8.07E+10	9.22E+09	8.84E+09	8.77E+09	8.78E+09
Length scale for dTr = 1	hr	1	2.48	4.71	5.24	4.45	4.60
Corresponding height (m)		2.70	1.09	0.57	0.52	0.61	0.59
Required height (m)	h	2.70	0.41	0.41	0.41	0.41	0.41
Grashof temp diff (K)	Th-Tc	4	75.33	10.92	7.95	12.99	11.73
Supp/ex temp diff (K)	Te-Ts	3	56.50	8.19	5.97	9.74	8.80
Temp diff scale for hr =6.59	dTr	1	0.053	0.366	0.503	0.308	0.341

Table 4.1 (cont.) Refrigerant properties and scaling factors

Fluid	Symbol	R134a	R124	R125	R142b	R152a
Density (kg/m3)	ρ	3.34	5.84	5.07	3.8	2.8
Viscosity (kg/m s)	μ	1.19E-05	1.15E-05	1.29E-05	1.34E-05	9.94E-06
Kinematic viscosity (m^2/s)	ν	3.57E-06	1.96E-06	2.00E-06	2.73E-06	3.55E-06
Specific heat (J/kg K)	c_p	982	774	800	845	1338
Conductivity (W/mK)	k	0.0136	0.0117	0.0138	?	?
Thermal diffusivity (m^2/s)	α	4.15E-06	2.59E-06	3.40E-06	?	?
Prandtl number	Pr	0.861	0.759	0.748	?	?
Ambient temp (K)	T	293	293	293	293	293
Coeff. thermal exp (/K)	β	3.41E-03	3.41E-03	3.41E-03	3.41E-03	3.41E-03
Grashof number	Gr	1.16E+10	1.16E+10	1.16E+10	1.16E+10	1.16E+10
Rayleigh number	Ra	9.95E+09	8.75E+09	6.80E+09	?	?
Length scale for dTr = 1	hr	2.62	3.90	3.85	3.13	2.63
Corresponding height (m)		1.03	0.69	0.70	0.86	1.03
Required height (m)	h	0.41	0.41	0.41	0.41	0.41
Grashof temp diff (K)	Th-Tc	63.85	19.25	20.04	37.34	63.14
Supp/ex temp diff (K)	Te-Ts	47.89	14.44	15.03	28.00	47.35
Temp diff scale for hr =6.59	dTr	0.063	0.208	0.200	0.107	0.063

Table 4.2 Scaling for R114 and design conditions

Cooling load	40 W/m^2			80 W/m^2		
	Full scale	Ratio f.s./m	Model	Full scale	Ratio f.s./m	Model
Length (m)	8.03	6.59	1.22	8.03	6.59	1.22
Width (m)	4.02	6.59	0.61	4.02	6.59	0.61
Height (m)	2.70	6.59	0.41	2.70	6.59	0.41
Kinematic viscosity (m2/s)	1.51E-05	9.74	1.55E-06	1.51E-05	9.742	1.55E-06
Velocity (m/s)	0.143	1.48	0.097	0.286	1.48	0.193
Floor area (m2)	32.3	43.4	0.744	32.3	43.4	0.744
Free supply air area (m2)	1.25	43.4	0.029	1.25	43.4	0.029
Volume flow rate (m3/s)	0.178	64.2	2.78E-03	0.357	64.2	5.56E-03
Volume (m3)	87.1	286	0.305	87.1	286	0.305
1 ac/h (m3/s)	0.024	286	8.48E-05	0.024	286	8.48E-05
Volume flow rate (ac/h)	7.4	0.225	32.8	14.7	0.225	65.6
Density (kg/m3)	1.2	0.163	7.35	1.2	0.163	7.35
Mass flow rate (kg/s)	0.214	10.5	2.04E-02	0.428	10.5	4.09E-02
Specific heat (J/kg K)	1005	1.42	707	1005	1.42	707
Grashof temp diff (K)	4	0.368	10.9	4	0.368	10.9
Supp/ex temp diff (K)	6	0.368	16.3	6	0.368	16.3
Cooling (W)	1,291	5.48	236	2,582	5.48	472
Heat gains/area (W/m2)	40	0.126	317	80	0.126	634
Ambient temp (K)	293	1.00	293	293	1.10	266
Coeff. thermal exp (/K)	3.40E-03	0.904	3.76E-03	3.40E-03	0.904	3.76E-03
Conductivity	2.61E-02	2.58	1.01E-02	2.61E-02	2.58	1.01E-02
Thermal diffusivity	2.16E-05	11.1	1.94E-06	2.16E-05	11.1	1.94E-06
Viscosity (kg/m s)	1.82E-05	1.60	1.14E-05	1.82E-05	1.60	1.14E-05
Prandtl number	0.701	0.881	0.796	0.701	0.881	0.796
Grashof number	1.15E+10	1.00	1.15E+10	1.15E+10	1.00	1.15E+10
Archimedes number	17.7	1.11	16.0	4.4	1.00	4.4
Rayleigh number	8.04E+09	0.875	9.18E+09	8.04E+09	0.875	9.18E+09
Reynolds number	2.55E+04	1.00	2.55E+04	5.11E+04	1.00	5.11E+04

Table 4.3 Properties and scaling factors for R114 mixed with air

Properties

% oxygen		0.0%	3.0%	3.5%	5.0%	6.5%	11.0%	20.80%
% air		0%	14%	17%	24%	31%	52%	100%
Density, kg/m^3	ρ	7.2	6.3	6.2	5.8	5.3	4.0	1.2
Dynamic viscosity, kg/m.s	μ	1.15E-05	1.19E-05	1.20E-05	1.23E-05	1.27E-05	1.42E-05	1.84E-05
Conductivity, W/m.K	k	0.0104	0.0110	0.0113	0.0121	0.0132	0.0173	0.0260
Specific heat, J/kg.K	c_p	713	756	763	785	807	871	1006
Thermal exp. coeff., 1/K	β	3.68E-03	3.63E-03	3.63E-03	3.60E-03	3.58E-03	3.50E-03	3.33E-03
Prandtl number	Pr	0.792	0.781	0.779	0.774	0.768	0.752	0.712
Kinematic viscosity, m^2/s	ν	1.6E-06	1.9E-06	1.9E-06	2.1E-06	2.4E-06	3.5E-06	1.6E-05

Scaling factors (full scale/model)

Density	ρ	0.164	0.187	0.191	0.205	0.222	0.294
Dynamic viscosity	μ	1.60	1.54	1.53	1.49	1.45	1.29
Conductivity	k	2.51	2.36	2.31	2.15	1.98	1.50
Specific heat	c_p	1.41	1.33	1.32	1.28	1.25	1.16
Thermal exp. coef.	β	0.90	0.92	0.92	0.93	0.93	0.95
Prandtl number	Pr	0.90	0.91	0.91	0.92	0.93	0.95
Kinematic viscosity	ν	9.7	8.3	8.0	7.3	6.5	4.4
Height	h	6.6	6.6	6.6	6.6	6.6	6.6
Temperature difference	dT	0.36	0.26	0.24	0.20	0.16	0.07
Velocity	v	1.5	1.3	1.2	1.1	1.0	0.7
Volume flow rate	Q	64	54	53	48	43	29
Mass flow rate	m	11	10	10	10	10	9
Power	q	5.4	3.5	3.2	2.5	1.9	0.7
Power intensity	q"	0.12	0.08	0.07	0.06	0.04	0.02

Table 4.4 Design conditions for R114 mixed with air at 40 W/m^2

	Model	Full scale equivalents					
Height (m)	0.41	2.70	2.70	2.70	2.70	2.70	2.70
Velocity (m/s)	0.068	0.1	0.080	0.082	0.091	0.101	0.150
Volume flow rate (m^3/s)	5.56E-03	0.357	0.0066	0.0068	0.0074	0.0083	0.0123
Mass flow rate (kg/s)	0.041	0.428	0.042	0.042	0.043	0.045	0.050
Grashof temp diff (K)	10.9	4	15.4	16.4	20.0	24.9	56.3
Supp/ex temp diff (K)	8.2	3	11.5	12.3	15.0	18.7	42.3
Cooling (W)	237	1,291	367	397	512	673	1,848
Heat gains/area (W/m^2)	317	40	494	6,600	113,591	2,572,641	159,941,060

	Full scale	Model equivalents					
Height (m)	2.70	0.41	0.41	0.41	0.41	0.41	0.41
Velocity (m/s)	0.1	0.068	0.085	0.082	0.075	0.067	0.045
Volume flow rate (m^3/s)	0.357	5.56E-03	0.30	0.29	0.27	0.24	0.16
Mass flow rate (kg/s)	0.428	4.09E-02	0.42	0.41	0.40	0.39	0.35
Grashof temp diff (K)	4	10.881	2.83	2.66	2.17	1.75	0.77
Supp/ex temp diff (K)	3	8.161	2.12	1.99	1.63	1.31	0.58
Cooling (W)	1,291	236	830	766	595	452	165
Heat gains/area (W/m^2)	40	317	26	24	18	14	5

5. Existing model

5.1 Box

An existing box was used for the scale model, with some modifications. The box was built by Doug Olson[6] for studying natural convection in enclosures at high Rayleigh number using a small scale model. The apparatus had been designed as a flexible experimental facility that could accommodate a variety of types of natural convection, forced convection or combined convection experiments in enclosures. By operating the experiments at atmospheric pressure and temperature, the wall elements were not required to withstand large forces or accommodate significant thermal expansion. Because of this, the walls were constructed out of composite materials, with low density, low thermal conductivity elements to reduce the thermal capacitance, heat loss and thermal coupling between walls. See figure 5.1. The ceiling and the floor were transparent so that the experiments could be observed. All the vertical walls could be heated and three of the four walls could be cooled, to allow for a variety of heat flux or temperature boundary conditions.

The model had been designed to use a scale of 1:5. The inner dimensions of the box were 136 cm long, 69 cm wide and 47 cm high. Each vertical wall was a composite structure consisting of three sections of aluminum plate, stacked one above the other. Closed-cell polyurethane foam insulation strips separated the plate sections. A strip of foam surrounded the outer perimeter of each wall to thermally isolate it from its neighbors. Aluminized mylar strips were glued on the inner facing side of the foam insulation strips to reduce the surface emissively. The edges and corners were sealed with a soft, closed-cell urethane foam gasket, coated with vacuum grease.

The additions to this apparatus were also designed, built and used by Mehmet Okutan[13] for a study into the effect on displacement ventilation of adding small fans to the space at low level.

5.2 Heating and cooling panels

Electrical resistance strip heaters were bolted to the back side of each wall section of the four vertical walls, with a thin layer of thermal contact grease between the plates and the heaters. Copper cooling tubes were soldered to the back side of the wall sections of the two side walls and one of the end walls.

5.3 Flow visualization

The velocity and behavior of the fluid could be observed by injecting a light reflecting smoke into the test cell and illuminating it with a planar light source. Olson had established that a suitable smoke for use with the dense R114 refrigerant gas was ammonium chloride. The injected smoke introduced negligible buoyancy into the natural convection flow. The smoke generator consisted of small jars (250 ml) of concentrated hydrochloric acid (HCl) and ammonium hydroxide (NH_3OH), filled about a quarter full. Each jar had a cap with two ports. R114 gas from an external tank was passed into the jar containing the acid at a low flow rate (1 - 3 ml/s), entraining the acid vapors. The gas then passed into the jar containing the ammonium hydroxide, where the acid vapors reacted with the ammonium chloride vapors to form a white smoke. The smoke-laden refrigerant was then injected into the test cell. A valve on the refrigerant supply tank provided control of the smoke flow rate, and the flow rate was measured using a flowmeter. The injection tube was rather

large (0.6 cm ID), to prevent clogging of the smoke and to keep the injection velocities small.

Olson used a slide projector to provide a vertical plane of light, oriented parallel to the primary direction of the flow motions. The projector was mounted in a rack above the test box. A slide was masked to provide a vertical slit of light and placed in the projector. The light was then directed at an angle downward through the ceiling. The video system consisted of a low light-level black and white camera, a 1/2" VHS recorder, a time-date generator and a black and white monitor.

The same apparatus had also been used by Frank Revi[14] for flow visualization to measure two-dimensional concentration fields of a glycol-based tracer aerosol. He used a dynamic laser light sheet produced using an oscillating mirror in conjunction with a charge coupled device (CCD) camera, microcomputer image acquisition hardware (a frame grabber board) and image processing software. The laser was mounted above the test box at the side and it was directed to the mirror of a scanner which was mounted directly above the test box, over the area of interest. A circular hole was cut in one end wall and a lens was inserted there. The camera was placed in front of this lens so that it was perpendicular to the sheet of light.

The laser was an Omnichrome air cooled argon laser, model 532. The wavelength used was 514 nm (green). The General Scanning Series G optical scanner consisted of a mirror and galvanometer, which were supported by a Melles Griot pivot structure. It was controlled by a Global Specialties function generator and a Realistic SA-10 solid state stereo amplifier. The scan angle used was approximately 15° to 30°. The camera was a Cohu CCD monochrome camera, model 6510. It consists of miniature camera head and a camera control unit (CCU). The camera head contains a 1/2" format charge coupled device image sensor and related support circuits. The active imaging area is 6.4 by 4.8 mm, with an array of 739 horizontal by 484 vertical picture elements.

The camera signal was fed into a Data Translation Quick Capture frame grabber board, producing 640 x 480 resolution with 256 (8 bits) levels of gray. An Apple Macintosh 2 computer was used to process the video data. Captured images were processed with NIH Image 1.40 software and stored in tagged image file format (TIFF). NIH Image is a public domain image processing and analysis program for the Macintosh. It can acquire, display, edit, enhance, analyze, print and animate images. Updates to Image are available to Internet users via anonymous ftp from alw.nih.gov. It was written by Wayne Rasband, Research Services Branch, National Institute of Mental Health.

Figure 5.1 Composition of box walls
(M. Okutan[13], Masters thesis, 1995)

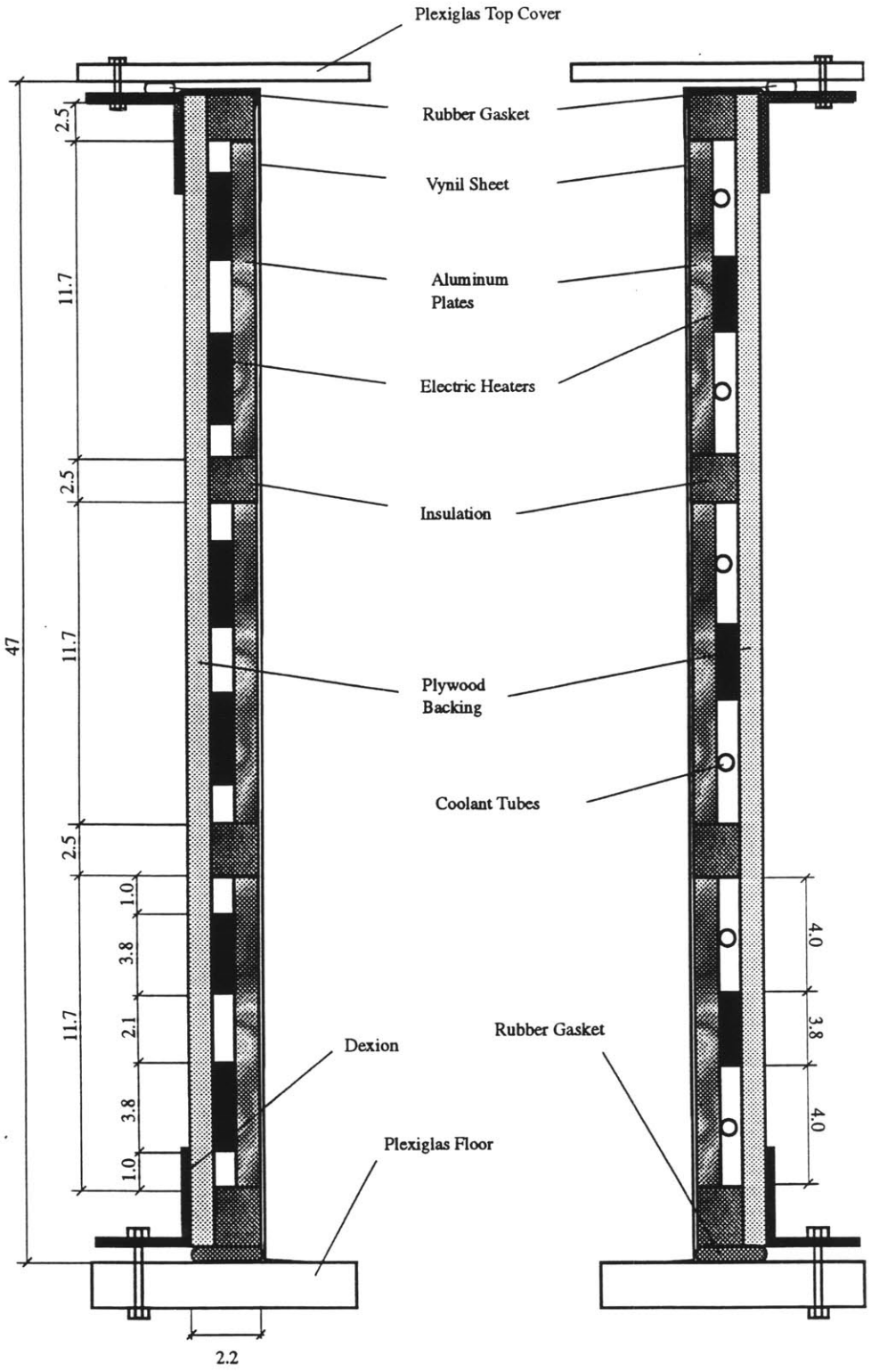

Figure 5.2 Refrigeration supply and smoke generation

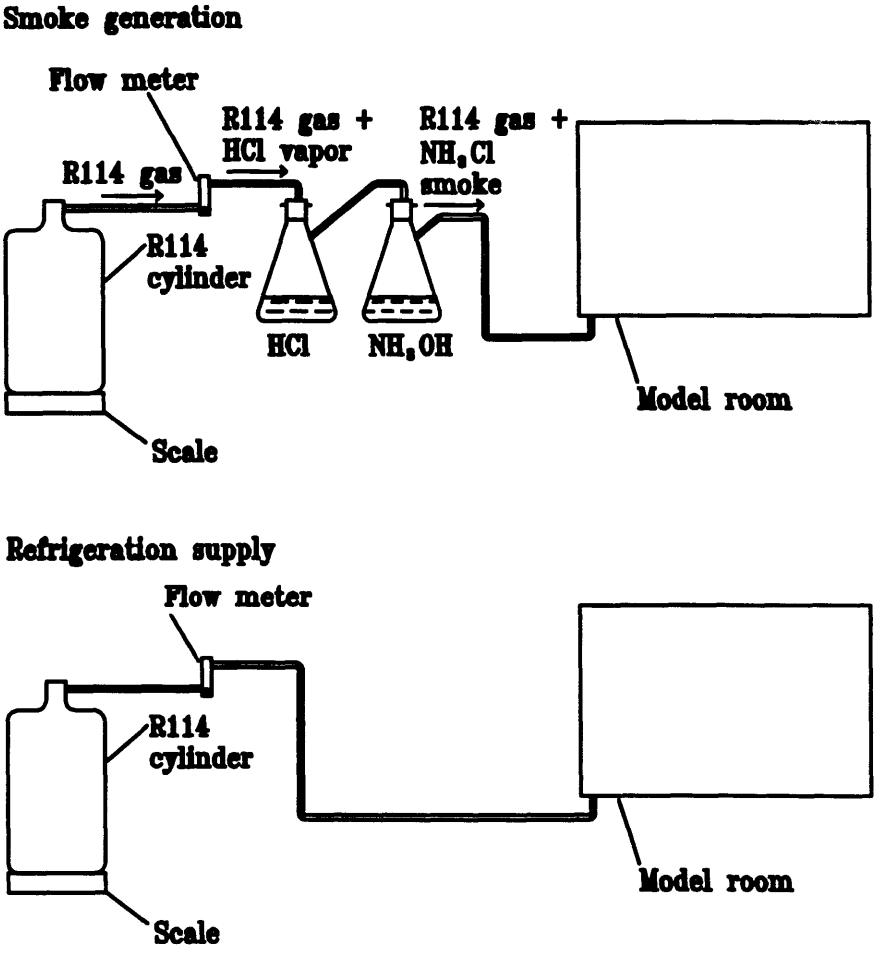

6. Design of gas and water circuits

6.1 Gas circuit

The gas circuit consisted basically of a fan and a heat exchanger, with a flow measuring device, shut off valves at the supply and exhaust tubes and bleed valves to be used when the box was filled with refrigerant. See figure 6.1. The major concern was to keep the pressure drop of the circuit low, because the available fans would have to operate very close to the end of their range to provide a large enough pressure drop at the required flow rate. The tubes were sized at 2", which gave a pressure drop of 11 Pa/m at design conditions. Tubes of 2 1/2" were considered, but they are a non-standard size, so the tubes and fittings are expensive and not readily available. Using 3" tubes would have been an over-design. Table 6.1 shows the pressure drop calculations for the gas circuit. Unions were placed in the supply and the exhaust legs so that the connections to the box could be removed easily, and between the fan and the heat exchanger so that the model could be moved and to enable checking the system.

6.2 Fan

Centrifugal fans were found to have the best characteristics for the purpose, providing relatively high pressures for a given flow rate, compared with axial fans. The fan selected had a maximum flow rate of 86 cfm with air. The model was A086 from Electro Sales and it was an OEM replacement for Rheem. It had its own speed controller, so no damper was needed to control the flow. A fan housing was designed out of 1/2" plexiglass, with dimensions 13" x 13" x 12". The sides were glued together using a plastic acrylic cement which worked by capillary action, drawing the glue into the space between the two pieces of plexiglass. The cover at the back could be removed, and it was sealed using a rubber gasket. It had two holes with Swagelock fittings inserted in them, for filling the housing with refrigerant at the bottom, letting air out at the top and connecting a manometer tube to take pressure measurements across the fan.

6.3 Heat exchanger

The largest pressure drop in the system was due to the heat exchanger. Initially, it was proposed the the gas be run through a large coil directly through a 50 gallon barrel filled with ice and water, which would be simple and cheap. It was found that the coil could not easily be manufactured if the tube diameter were larger than 1 1/2", and at that size, it's length would have to be 91 ft, with a corresponding pressure drop of 22 in wg, which was much too high for any available fans. It was also estimated to cost $450. Therefore, a conventional heat exchanger was chosen instead. It was still difficult to find one that had a low enough pressure drop for the flow. The one selected was a Basco shell and tube heat exchanger, no. 05014, from American Industries Inc.. The quoted pressure drop was 0.02 psi or 0.55 in wg, 138 Pa through the tubes on the gas side at design conditions, with a heat transfer of 470 W. For the water side, the shell pressure drop was 0.1 psi, 2.8 in wg, 690 Pa. It cost $480.

Table 6.1 Pressure drop calculations for gas circuit

				2", R114 40 W/m2	2", air equivalent	2", R114 80 W/m2	2" ratio air / gas	2", air equivalent	2 1/2", R114 80 W/m2	3", R114 80 W/m2
ow rate, m^3/s				5.56E-03	5.56E-03	1.11E-02		1.11E-02	1.11E-02	1.11E-02
ow rate, cfm				11.8	11.8	23.5		23.5	23.5	23.5
y, kg/m^3				7.35	1.2	7.35	0.163	1.2	7.35	7.35
ity, kg/m s				1.137E-05	1.82E-05	1.137E-05	1.601	1.82E-05	1.137E-05	1.137E-05
ter, in				2.0	2.0	2.0		2.0	2.5	3.0
ter, m				0.0508	0.0508	0.0508		0.0508	0.0635	0.0762
sect. area, m^2				2.03E-03	2.03E-03	2.03E-03		2.03E-03	3.17E-03	4.56E-03
ty, m/s				2.74	2.74	5.49		5.49	3.51	2.44
lds number				9.01E+04	9.19E+03	1.80E+05	0.102	1.84E+04	1.44E+05	1.20E+05
n factor f'				0.0211	0.0329	0.0194	1.451	0.0282	0.0193	0.0194
n loss, Pa/m				11	3	42	0.237	10	14	6
of tube, m				3.85	3.85	3.85		3.85	3.85	3.85
re drop, tube, Pa				44	11	163	0.237	39	53	21
re drop, tube, in wg				0.18	0.05	0.65	0.237	0.15	0.21	0.09
re, fittings, in wg				0.81	0.13	3.24	0.163	0.53	1.33	0.64
re, HE, psi				0.02	0.005	0.02	0.273	0.005	0.02	0.02
re, HE, in wg				0.55	0.15	0.55	0.273	0.15	0.55	0.55
re, circuit, in wg				1.54	0.33	4.45	0.188	0.84	2.09	1.28
^2				27.65	4.52	110.69	0.163	18.07	45.34	21.86
ngs	k	No.	Comb.k	Pressure drop for fittings, Pa						
elbow	0.38	4	1.52	42	7	168	0.163	27	69	33
nch	0.84	2	1.68	46	8	186	0.163	30	76	37
lve	0.34	2	0.68	19	3	75	0.163	12	31	15
	0.1	4	0.4	11	2	44	0.163	7	18	9
, 1 outlet box, fan	1	3	3	83	14	332	0.163	54	136	66
for fittings, Pa			7.28	201	33	806	0.163	132	330	159

Figure 6.1 Gas circuit schematic

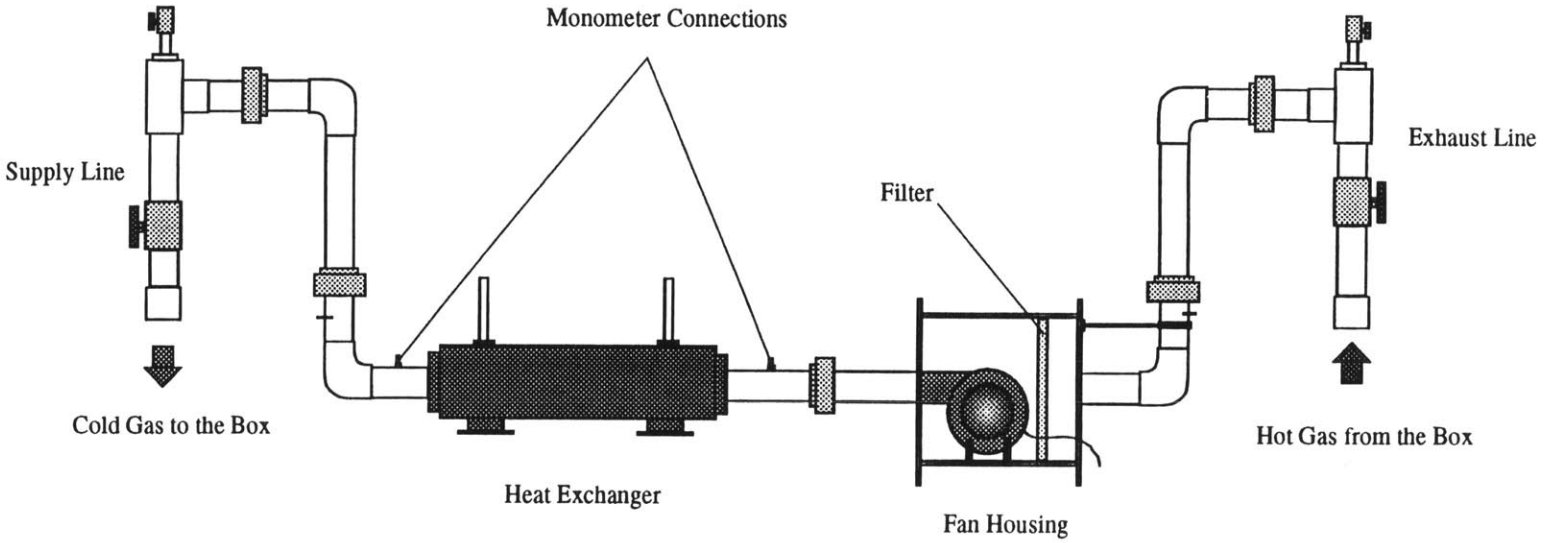

Figure 6.2 Water circuit schematic

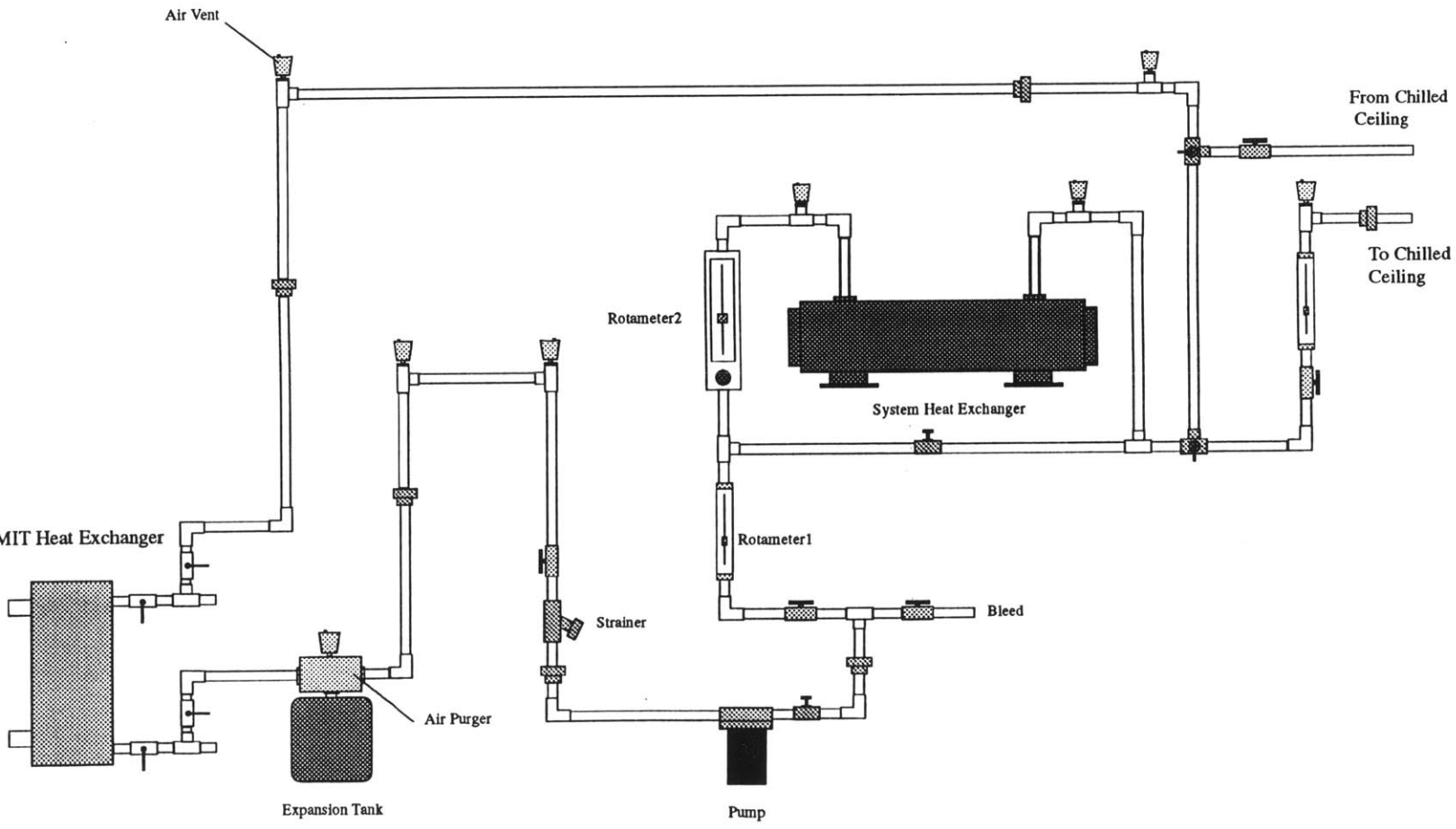

6.4 Water circuit

The water circuit consisted of a heat exchanger connected to the MIT cooled water circuit, a pump with a needle valve to control the flow in the main circuit, the gas/water heat exchanger with a flow and bypass loop to control the flow through the heat exchanger and a serpentine coil on the radiant panel with a flow and bypass loop. See figure 6.2. There were two flow meters (rotometers), one in the main circuit, which measured the flow rate up to 5 gpm, from Blue White Industries, and the other in the heat exchanger loop for up to 20 gph, from Dwyer. There were air vents at the top of each riser, to vent air from the system, a drain at the bottom of the circuit, on the discharge side of the circuit, so that the pump could be used to help empty the system, and a strainer with a ball valve on the suction side of the pump, to remove any dirt and debris in the system. An expansion tank was fitted to allow the water in the system to expand and contract without damaging the pipes and fittings. It was placed on the suction side of the pump so that the whole system would be above atmospheric pressure. The expansion tank pressure was 12 psig and could be altered if required.

6.5 Pipework

The pipes were sized at 1/2" which gave a low pressure drop and was a convenient size to fit the pump and some of the fittings. 1'2" pipes and fittings were readily available. They were all PVC, apart from at the connection to the cooling supply. PVC was much easier to assemble than copper, as it could be glued together, rather than soldered. Unions were used in several places, so that the pipework could be dismantled easily when the model was moved for repairs or for design changes.

6.6 Pump

The pump selected was a Laing brass recirculating pump, SM-303. The maximum pump pressure was 6.5' inches of water and the maximum flow rate was 4 gpm at 2' in wg. Its design operating condition was 0.4 gpm at 6.4' in wg.

6.7 Chilled water supply

The laboratory had a cooling water supply from the MIT system. A separate heat exchanger for our system permitted it to be independent of the MIT system, not on the primary circuit. There was a possibility that other students would want to use this water supply for different experiments, so our system was designed with additional taps. However, no use was planned for the duration of our experiments, so the simplest circuit was designed. This meant that instead of having primary and secondary loops, each with their own pump, there was a fixed system with just one pump. Another experiment could be run, with its own pump, but not at the same time. The MIT heat exchanger could provide 6166 W of cooling with a maximum flow rate of 3 gpm, which was ample for our purposes. The pressure drop at this rate was 0.4' or 4.8" water. On the MIT side, the maximum flow rate and pressure drop were the same, the design chilled water entering temperature was 43 °F or 6.1°C and the design leaving temperature was 57 °F or 13.9°C.

6.8 MIT Heat Exchanger

The connections to the MIT heat exchanger were 1" copper. Unions were used at the inlet and outlet so that the circuit could easily be changed in the future. The pipes were silver soldered. One inch valves and caps were left for another user to tap off, and 1/2" pipes for our system were taken off the 1" pipes using reducing tees which help to balance the take-offs. Unions were added here for flexibility and to provide the threaded connection to change over to PVC.

7. Inside of model

7.1 Walls, ceiling and floor

False walls and a false ceiling and floor were put into the test box, made of clear plexiglass. See figure 7.1. They allowed the fluid to be supplied at the top of the test box through an opening in the top cover, directed to enter the model room from the side wall. In the future, the walls could be modified to supply fluid through the floor. The fluid was extracted through grilles in the ceiling to the exhaust tube in the top cover. A new top cover was made with holes for the supply and exhaust connections. The inside dimensions of the room were then 122 cm long, 61 cm wide and 41 cm high. The height of the full scale room which was being modelled was determined to be 2.7 m for a typical office, so the scaling factor was set at 6.6. This meant that the length and width of the full scale room were 8.0 m and 4.0 m, which were the same dimensions as for the Olsen/Ferm[1] study. The outside walls and the bottom of the box were insulated with 100 mm thick glass fibre insulation. The top was insulated with 25 mm extruded polystyrene, R value 5.0.

7.2 Grilles

Grilles were formed by attaching perforated aluminum sheet with 42% free area to holes cut in the walls. For the supply, there were two grilles or diffusers in the long side wall, each 12 by 12 cm, which corresponded to 0.78 by 0.78 m for the full scale case. The pressure drop across the grilles was calculated to be insignificant . There were two exhaust grilles in the ceiling, each 4 by 4 cm, corresponding to 0.26 by 0.26 m.

7.3 Heat sources

Heat sources were put in the room to simulate a real office with people, computers, xerox machines and lights. Cylindrical electrical resistances were placed inside aluminum enclosures. The enclosures were rectangular for the machines and cylindrical for the people. The lights were suspended from the ceiling uncovered. See table 7.1 for the dimensions of the models and their full scale dimensions. The models included three workstations with three people, three computer screens, three computer towers, three xerox machines on tables and three lights suspended from the ceiling. The occupant density was up to 1 person per 11 m^2, which is a little better than the generally recommended 1 per 10 m^2. The person in the middle was made up of two shorter cylinders to simulate someone sitting down. The three computer screens and the xerox machines were placed on tables made out of cardboard so that they were at roughly a realistic height, and the other three machines were placed on the floor to simulate processors.

Table 7.1 Dimensions of heat sources at model and full scale

	Model dimensions, cm				Full scale dimensions, m			
Description	Length	Width	Height	Dia.	Length	Width	Height	Dia.
Person standing			27.0	5.0			1.78	0.33
Person sitting down		(2 x)	11.0	5.0		(2 x)	0.73	0.33
Computer screen	8.3	5.1	4.3		55	34	28	
Computer tower	4.0	5.2	10.2		26	34	67	
Xerox machine	13.3	7.3	5.3		88	48	35	
Light	10.0			1.5	66			10

Figure 7.1

Layout of heat sources in model room

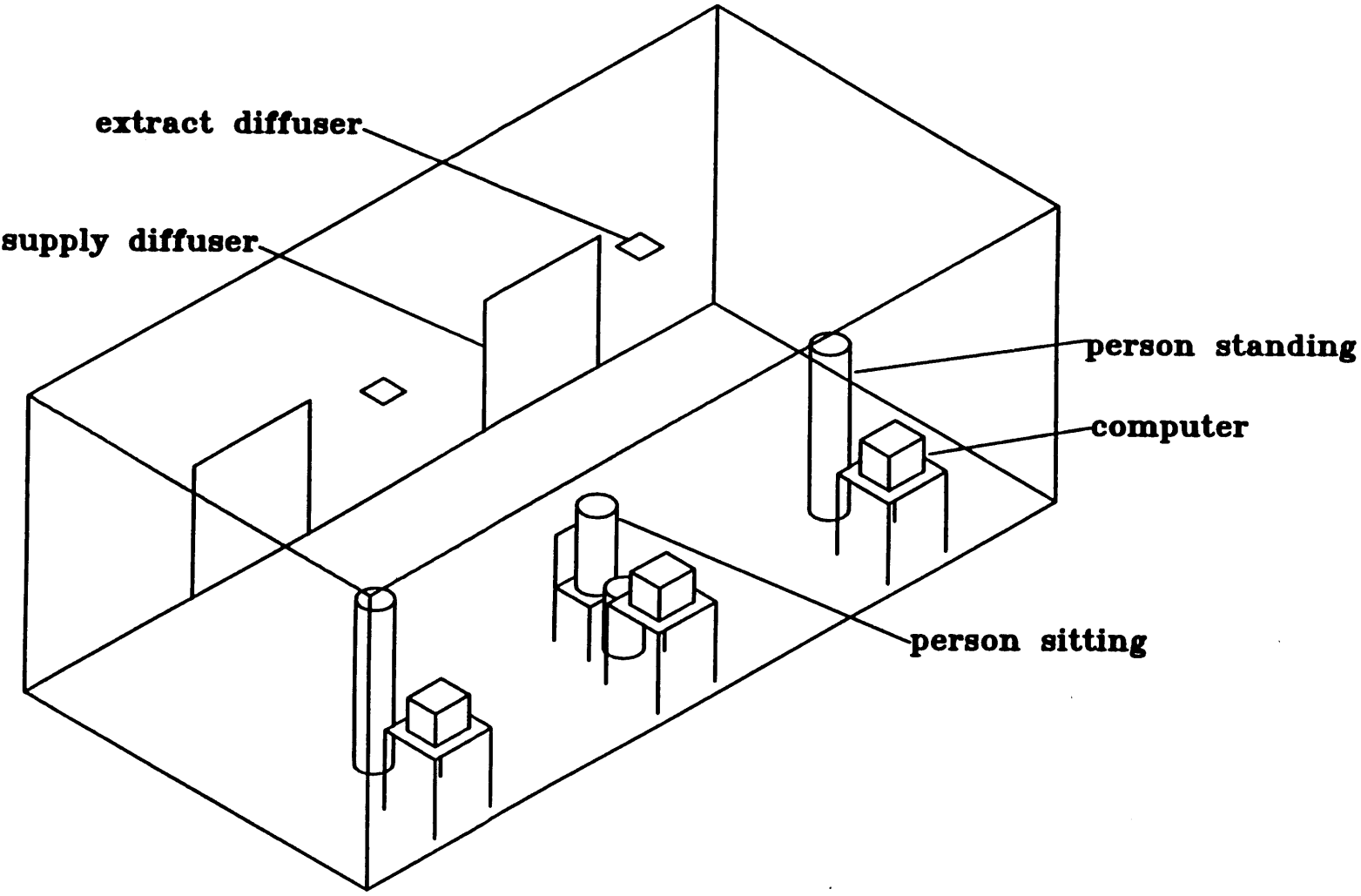

Figure 7.2 Plan of layout of heat sources in model room

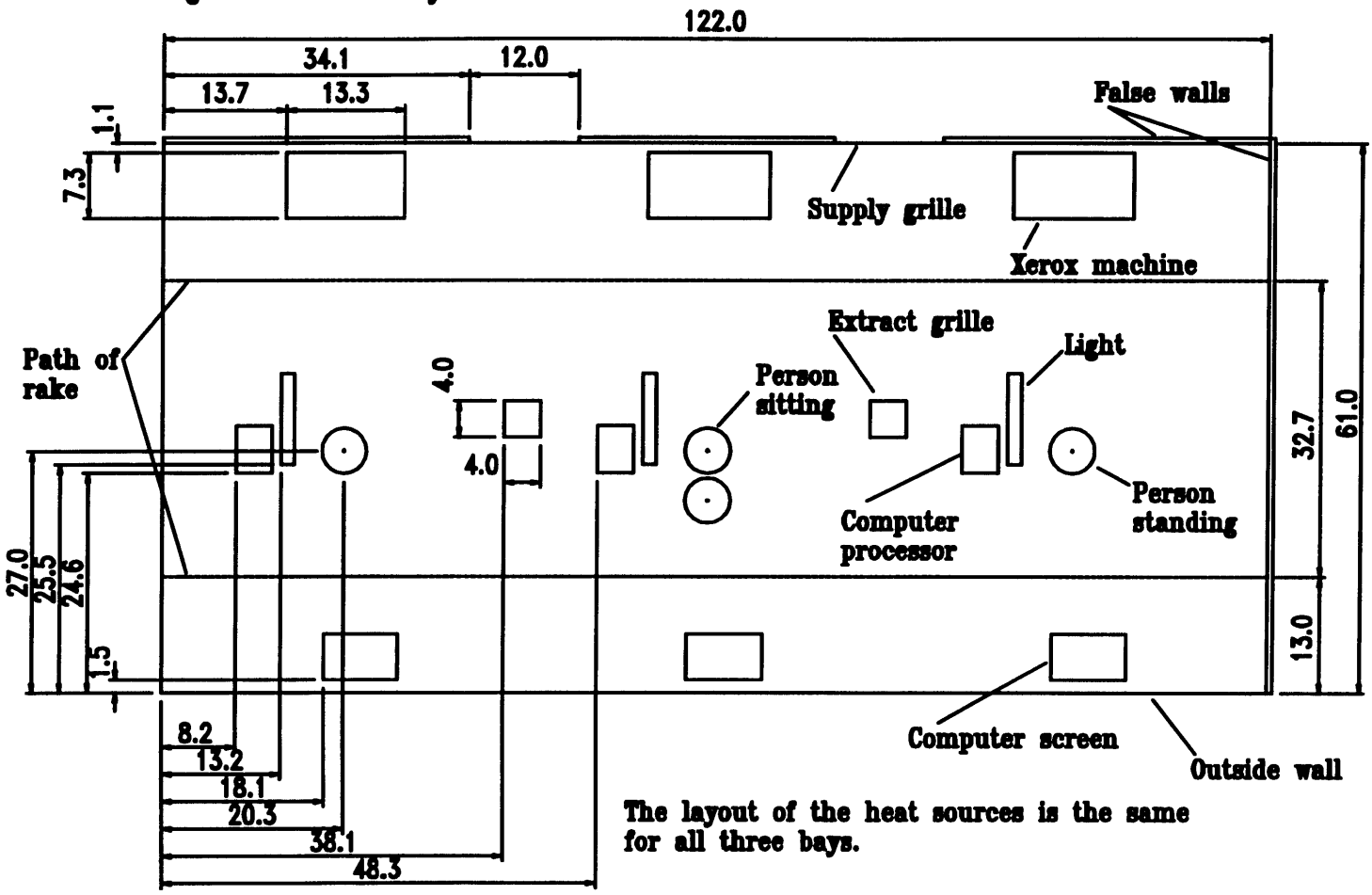

The layout of the heat sources is the same for all three bays.

7.4 Electric circuits

The resistances and voltage supplies were chosen such that the power out of these heat sources matched real power outputs when scaled, i.e., 100 W sensible heat for the people, 100 W for the computers, 180 W for the xerox machines and 160 W for the lights. Each of the people and machines could be heated independently and their power inputs could be varied. The lights could be controlled together. See table 7.2 for the power output settings for full scale simulations of between 20 and 60 W/m^2 with the model heat sources alone and for up to 100 W/m^2 with the heated side wall.

Table 7.2 Power outputs of heat sources for the model and full scale equivalents

Full scale					Model					
Area ~32 m^2	Intensity,	Power,	Number	Power,	(f.s. power/5.48)		Resistance/	Volts/	Volts/	%supply
Heat gains	W/m^2	W	of items	W/item	W/item	W	item, ohms	item	circuit	110V
People	10	320	3	107	20	59	150	54	54	49
Computer screens	9.4	300	3	100	18	55	150	52	52	48
Xerox machines	5.6	180	1	180	33	33	150	70	70	64
Lights	15	480	3	160	29	88	10	17	51	47
Total	40	1280	10			234				
People	10	320	3	107	20	59	150	54	54	49
Computer screens	18.8	600	6	100	18	109	150	52	52	48
Xerox machines	11.3	360	2	180	33	66	150	70	70	64
Lights	15	480	3	160	29	88	10	17	51	47
External (window)	25	800	1	800	146	146	6.5	31	31	28
Total	80	2560	14			467				
People	6.7	214	2	107	20	39	150	54	54	49
Computer screens	3.1	100	1	100	18	18	150	52	52	48
Lights	10.2	326	3	109	20	59	10	14	42	38
Total	20	640	10			117				
People	10	320	3	107	19	58	150	54	54	49
Computer screens	9.4	300	3	100	18	55	150	52	52	48
Xerox machines	5.6	180	1	180	33	33	150	70	70	64
Lights	15	480	3	160	29	88	10	17	51	47
External (window)	20	640	1	640	117	117	6.5	28	28	25
Total	60	1280	10			350				

8. Design of cooled ceiling

8.1 Panel

There are two main types of cooled ceiling, radiative and convective. The radiative type was chosen for this study. See Figure 8.1. It was a 1.2 m x 0.6 m modular panel from Frenger, Alberta, Canada. It consisted of copper tubes mechanically fastened to an aluminum tray. The tubes were 1/2" I.D. and they were formed into a 6-pass serpentine coil. Thermal contact between the coil and the panel was maintained by a non-hardening heat conductive paste and held in place by an aluminum retainer fastened with stud-welded aluminum bolts. The tray was made form 18 gauge or 1 mm thick aluminum sheet with the edges folded at right angles. The finish was off-white paint. The coils were covered by a 25 mm thick blanket of foil-backed fiberglass insulation.

8.2 Water supply

The copper tubes were connected to the remainder of the water system with 1/2" copper fittings, silver soldered together. Unions were used to connect the copper to the PVC system. The flow through the ceiling was controlled by a flow and bypass arrangement and measured with a 0.1 - 1 gpm in-line rotameter. The temperature of the supply water was increased by wrapping a flexible electric resistor heater round the supply pipe. For a full scale system, the average water temperature is kept at a minimum of 16°C to avoid forming condensation on the ceiling. The water temperature was scaled to provide an average temperature of the equivalent of 16°C. The panel was rated at 9.6 W/K of temperature difference, e.g. for a room average temperature of 22°C and a water supply temperature of 10°C, the cooling capacity is 115.2 W/m^2. For the model, a typical actual water supply temperature was 15°C.

Figure 8.1 Diagram of cooled ceiling panel

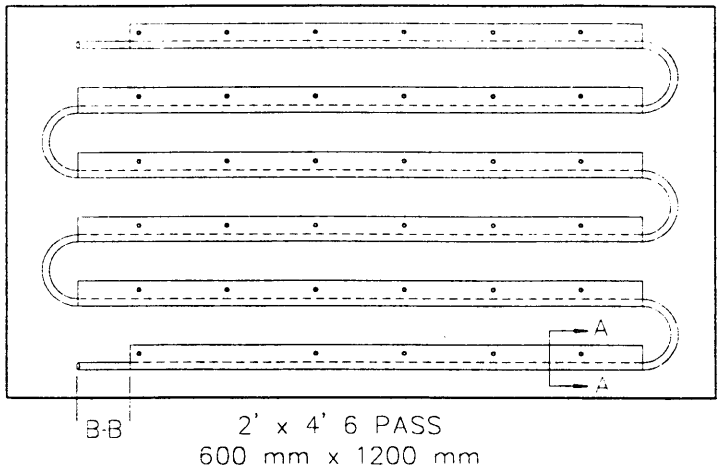

VIEW B-B

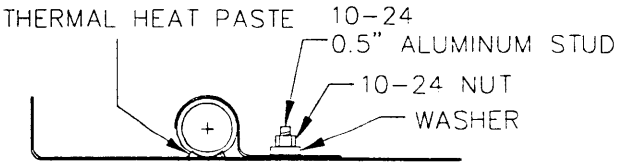

SECTION A-A

9. Gas flow measurement

9.1 Calibration

The original design used a flowmeter to measure the flow rate of the gas. However, when the fan was turned on, the pressure drop across the flowmeter was so large that there was virtually no flow. The flowmeter was taken out and replaced by straight tubing. Instead, the flow rate was calibrated by running air through the system and measuring the pressure drop across the heat exchanger. The heat exchanger was chosen because it caused the largest pressure drop in the system and this pressure drop could be modelled analytically.

The flow rates were measured using a hot-wire anemometer and a Solomat MPM 500e multi-functional instrument. The probe was a 129MS hot wire thermistor. It read the velocity of the air. The 2" tube was opened at a union and readings were taken by traversing the tube in two perpendicular directions. The readings were averaged and the corresponding flow rate was calculated. The pressure drops were measured using a manometer connected to the 2" tubing at the inlet and the outlet of the heat exchanger. The ranges of measurements were from 9.9 - 15.2 m/s, 20.1 - 30.8 l/s and 0.29 - 0.64 "wg.

9.2 Dimensional analysis

The measured values were converted to equivalent values for refrigerant by using dimensional analysis. The dimensionless numbers used were the Euler number, Eu, which is the ratio of measured pressure to dynamic pressure, and the Reynolds number, Re_d, based on the diameter of the 2" tubing.

$$Eu = \frac{\Delta p}{\frac{1}{2}\rho\, v_t^2} \qquad \text{and } Re = \frac{\rho\, v_t\, d}{\mu}$$

The corresponding velocities and pressures were found by matching these dimensionless numbers., i.e.:

$$v_g = \frac{\rho_a\, v_a\, d}{\mu_a} \times \frac{\mu_g}{\rho_g\, d} \qquad \text{and } \Delta p_g = \frac{\Delta p_a}{\frac{1}{2}\rho_a\, v_a^2} \times \frac{1}{2}\rho_g\, v_g^2$$

In this case, the diameter, d, was unchanged. The ranges of scaled values for the refrigerant were 1.26 - 1.94 m/s, 2.6 - 3.9 l/s and 0.025 - 0.052 "wg. However, the required range for the flow rate was up to 12 l/s. Therefore, the data had to be extrapolated.

9.3 Empirical formula

The theoretical pressure drop across the heat exchanger was calculated for both air and R114. It depended on density, viscosity, the diameter of the heat exchanger tubes, roughness and length of heat exchanger. It consisted of the friction loss and losses at the inlets and outlets of the heat exchanger tubes and the 2" tubes.

The formula used was:

$$\Delta p = \left(k_{HE} + \frac{f\,l}{d}\right)\frac{1}{2}\rho\, v_{HE}^2 + k_t \frac{1}{2}\rho\, v_t^2 \qquad \text{where } f = 0.11\left(\frac{\varepsilon}{d} + \frac{68}{Re}\right)^{0.25}$$

The heat exchanger had 80 tubes, each with a diameter of 9.5 mm, and they were 0.3556 m long. The roughness factor was assumed to be 0.03 mm. The loss coefficients for the inlet and outlet to the heat exchanger were 1.0 each and for the 2" tubes they were 0.17 each. This formula did not give the values measured for air, so the constants were changed until the calculated values matched those measured for air and scaled for the refrigerant. It was found that changing the roughness had very little effect and the pressure loss due to the 2" tube inlet and outlet was negligible. The formula fit the data well with the length set to 1.5 m. Figure 9.1 shows a plot of Euler number versus Reynolds number for the calculated values over a range of flow rates as well as the measured data. Figure 9.2 shows a graph of pressure drop versus flow rate with the calculated values for both air and refrigerant, the measured values for air and the scaled values for refrigerant. The formula was also used to calibrate the heat exchanger for refrigerant containing some air, using the properties of the mixture as described in Chapter 4. See table 9.3.

Figure 9.1 Heat exchanger calibration - non-dimensionalized graph of pressure vs. velocity for measured and calculated values of air and R114

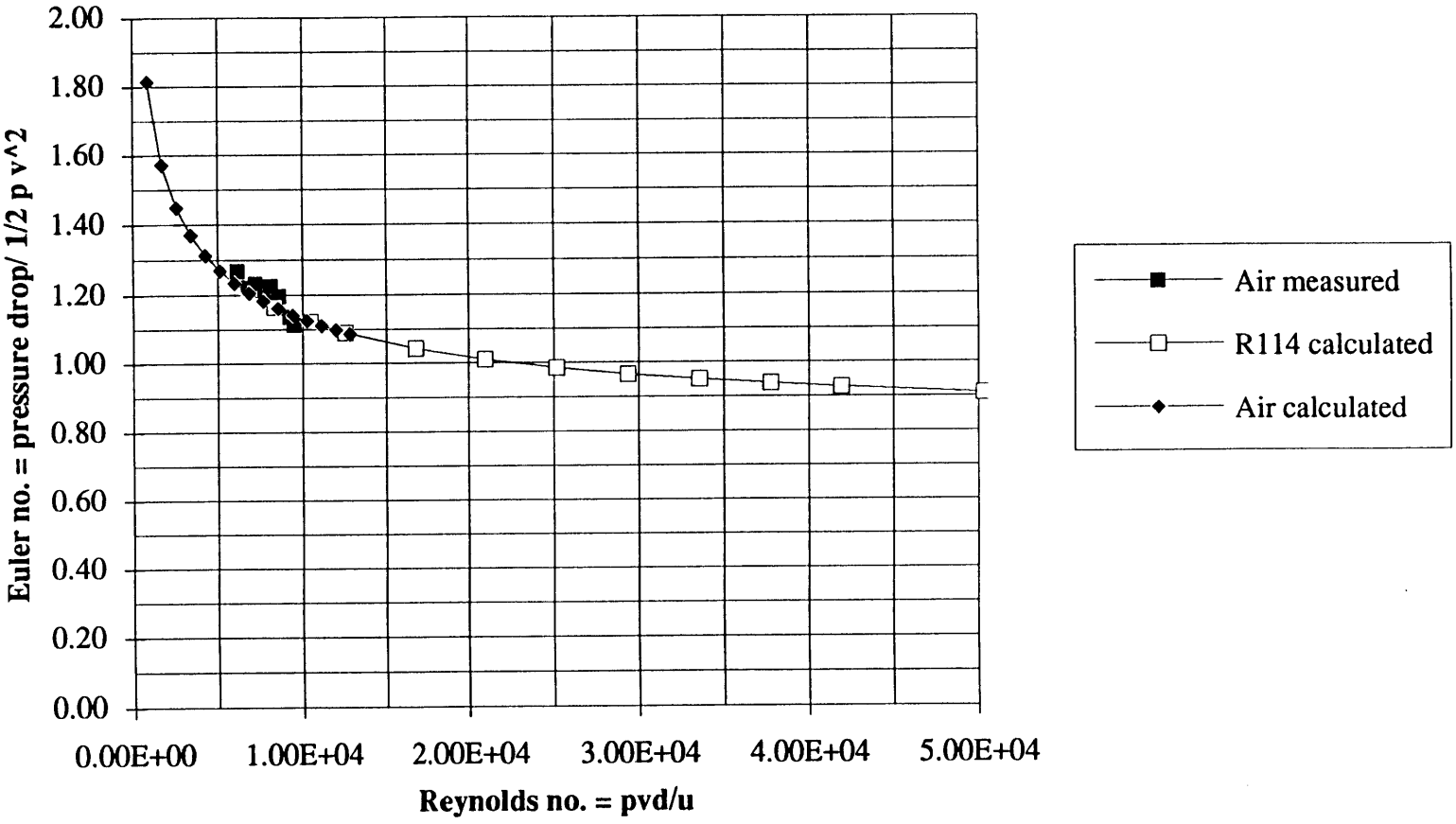

Figure 9.2 Heat exchanger calibration -
graph of pressure vs. flow rate for measured and calculated values of air and R114

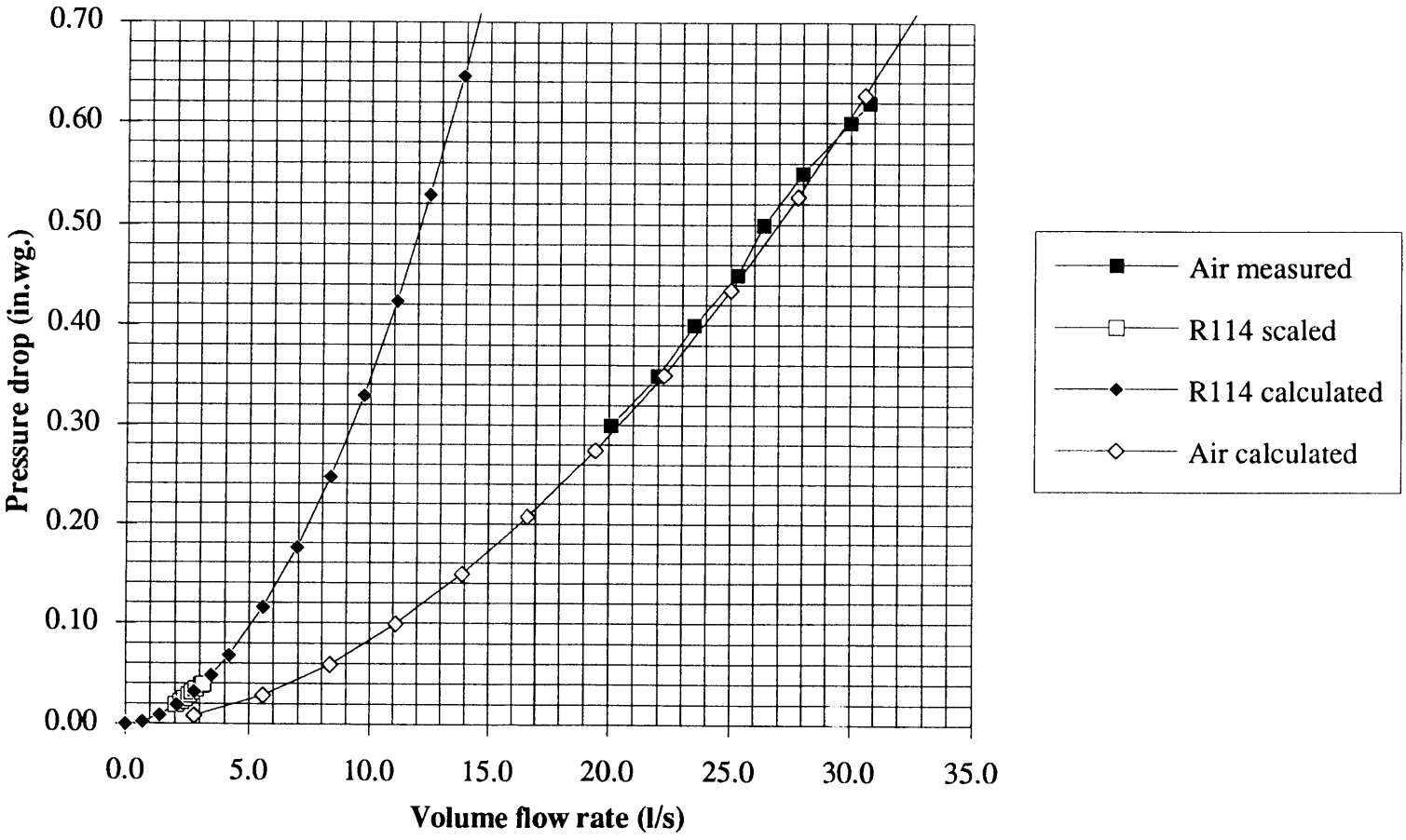

Figure 9.3 Heat exchanger calibration -
graph of pressure vs. flow rate for calculated values of mixtures of air and R114

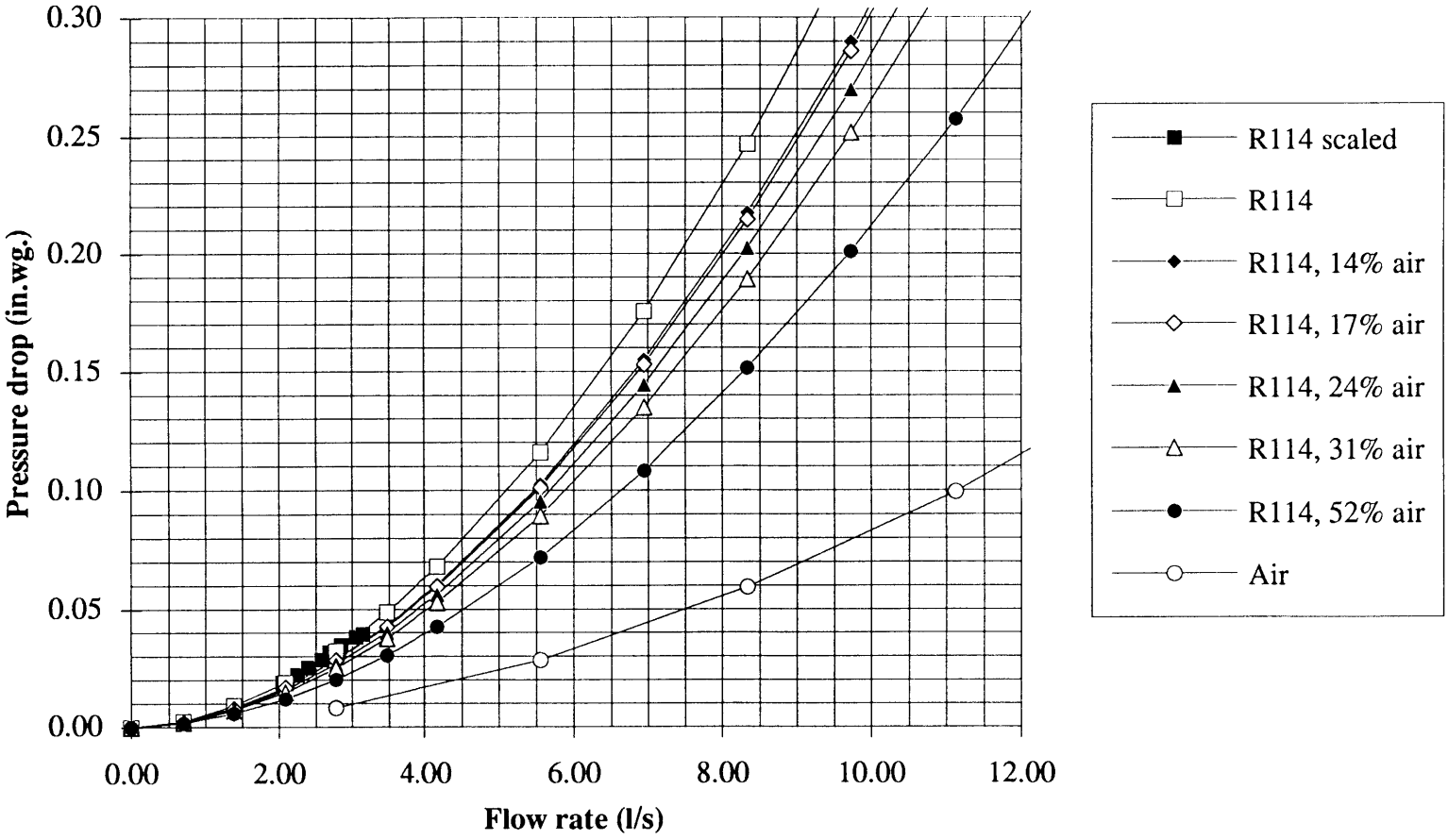

10. Temperature Measurement

10.1 Thermocouple rake

Thermocouples for measuring the temperature of the fluid were attached to two rods, which were supported by a movable rake. There were eight thermocouples per rod and they were located at heights of interest. See table 10.1. The channel numbers refer to the data acquisition channels. The column by the wall is nearer the outside side wall and the column by supply is nearer the supply diffusers. The thermocouples were T-type copper / constantine, which have a limit of error of 1.0°C or 0.75% over 0°C and a useful temperature range of -200 to 350°C. They were 36 gauge so that they would respond quickly to changes in temperature and not be too bulky in the space. They had PFA Teflon insulation, which meant that the maximum temperature was reduced to 260°C. The rods were plexiglass, chosen so that there would be negligible conduction of heat along the rods which would affect the temperatures around the rods being measured. The cross piece of the rake was an aluminum bar which was selected because it was stiffer than plexiglass and heat conduction horizontally was less significant at that height. It was supported by two fixed steel rods and it supported the end of the movable rod, which was hollow and contained the thermocouples.

Table 10.1 Heights of thermocouples on rake

Description	Full scale heights, m	Model heights, mm	Channel no., column by wall	Channel no., column by supply
Near extract	2.4	365	0	15
Above head	2.0	300	1	14
Head level for person standing	1.7	260	2	13
Head level for person sitting down	1.1	170	3	12
Sandberg[8] study	0.85	130	4	11
Center of gravity of person	0.6	90	5	10
Knee level	0.3	45	6	9
Ankle level	0.1	15	7	8

10.2 Data acquisition unit

The thermocouples were connected to terminals fixed to the rod outside the box and then extended using thicker 20 or 24 gauge thermocouple wire, also with PFA Teflon insulation, to a data acquisition unit (DAU). This unit consisted of two EXP-16 multiplexer boards which had 16 input channels per board and a cold junction compensator (CJC) for measuring temperature using thermocouples. The multiplexer boards were connected to a DAS-16G high-speed analog and digital interface board which was installed in an IBM 286 computer. The EXP-16 multiplexes the 16 differential analog input channels into one analog input of the DAS-16G data acquisition board. The cold junction sensing and compensation circuitry provides a scaling of 24.4 mV/°C, corresponding to 10 bits/°C on a 12-bit A/D converter. The DAS-16G could accept up to four EXP16 boards, providing a total of 64 channels of measurement, but in this case, only two boards were used, providing 32 thermocouple measurements.

10.3 Software

Fully integrated data acquisition software packages could not be used with this arrangement. Standard software written in Quick Basic, that was provided with the DAS-16G, was adapted to read inputs from both boards, convert the inputs from voltage to temperature measurements, average them, scale them and print them to the screen or write them to a file in DOS. The information on the file was then transferred to a Microsoft Excel spreadsheet using the "Apple File Exchange" to convert from DOS to Macintosh. It created columns of data from the numbers which were separated by commas. The spreadsheet was then used to provide charts of the results.

10.4 Thermocouple calibration

The error in repeatability of the EXP16 board with T-type thermocouples was ±1.9°C. this error was reduced to ± 0.5°C by averaging the readings 250 times. The thermocouples were calibrated by placing them in a beaker containing a mixture of ice and water. The outputs of the data acquisition unit were altered so that the thermocouples read 0°C, by adding offsets to the readings in the data acquisition program. The calibration was checked using a Pt 100 platinum RTD probe and a Solomat MPM 500e measuring instrument. The accuracy of this probe was ±0.5°C. The probe and the thermocouples were placed in water at room temperature and in hot water. The thermocouple readings agreed with the Pt 100 probe to within ± 0.5°C. The temperatures were scaled using a reference temperature of 19°C, which was the design supply temperature. This reduced the uncertainty of the temperature measurement to ± 0.15°C.

Reading $T_{full\ scale} = (T_{model} - 19) \times 0.36 + 19$

Error $\Delta T_{full\ scale} = \Delta T_{model} \times 0.36$

where 0.36 is the temperature difference scaling factor for R114 with no air and a height/ length scale of 6.6 (see table 4.3).

10.5 Model surface temperature measurements

The temperatures of the internal walls of the model were measured using the same type of thermocouples as on the rake. The wires were taped to the plexiglass surfaces so that the thermocouple bead touched the surface and some "Omegatherm" high thermally conducting paste was added to the bead to ensure good thermal contact. There were two thermocouples on the side wall, one on the end wall, two on the floor and two on the ceiling. There was also one at the back of each diffuser, to measure the temperature of the gas as it entered the room. The thermocouples for reading temperatures at the side and end external walls were 24 gauge T-type. The thermocouple in the side wall was between the wall heater, so it measured the heated wall temperature. These thermocouples were fixed in the original box, so they could not be put into the ice and water mixture. They were calibrated using the Pt 100 probe, which was held on the surface at each thermocouple location.

10.6 Gas and wall temperature measurements

The gas and the water thermocouples were 20 gauge T-type, which were much more sturdy than those on the rake and measuring the inside surfaces, but they had a slower response

time. This did not matter because they were being used to take readings at steady state. The thermocouples used for measuring the gas supply and return temperatures were inserted into the tubes through small holes, which were sealed using an epoxy glue. They were also calibrated using the Pt 100 probe. The water temperatures were read by taping thermocouples to the outside of the PVC pipes. The thermocouples were wrapped with insulation so that the surface temperatures of the pipes would be close to those of the water. It was estimated that the difference between the surface and water temperatures would be about the same for both the supply and the return pipe, so that the difference between the supply and return water temperatures would be about the same as those at the surfaces.

11. Use of Refrigerant

11.1 Leak testing

The box was tested for leaks by pressurizing it to 1.8 "wg or 450 Pa. This was done by running the fan at maximum speed with the valve on the return tube closed. The maximum working pressure was 0.55" or 140 Pa. A manometer was connected to the bottom of the box and its other connection was left open, to measure the difference in pressure between the inside of the box and the outside. Leaks were detected by injecting a small amount of refrigerant into the box and using a halogen detector. The gas tubing, heat exchanger and fan housing were also tested for leaks by connecting the whole system and running the fan. The pressure could be measured at the fan inlet and at the heat exchanger inlet and outlet. Refrigerant could also be supplied at the fan inlet.

11.2 Filling the box

The box was filled with refrigerant by supplying it slowly at low level and displacing the air, which was vented at the two highest points of the tubing, on the supply and the return sections. Initially, the box was raised about 10 cm at the end with the return tubing, using a car jack. The tubing was disconnected at two unions and stoppers were used to stop any gas from escaping. As the gas was much denser than air, it was assumed that it would form a layer at the bottom of the box, which would gradually increase in height. The supply rate to the box was approximately 230 l/h and it was estimated that it would take 2 hours to fill the box. The actual amount of refrigerant supplied was measured by weighing the cylinder containing the refrigerant and noting the change in weight. The box contained about 7 lbs of refrigerant when it was full. Once refrigerant was detected at the supply section vent, the valve there was closed. When refrigerant was detected at the return section vent, that valve was closed. The box was lowered and the tubing was connected to the rest of the gas system. Then the refrigerant was supplied at the bottom of the fan housing and air was vented at the top of the fan housing. When the housing was full of refrigerant, air was vented from the two high points as before and the heat exchanger and the tubing were slowly filled with refrigerant. It was found that the last amount of air was eliminated more efficiently when refrigerant was supplied to both the box and the fan housing at the same time. About 1.5 lbs of refrigerant was required to fill the gas system.

11.3 Oxygen monitoring

When it was estimated that the box and gas system were full, the amount of oxygen remaining inside was measured using a Bacharach Fyrite II combustion efficiency analyzer. It read the percentage of oxygen in the sample. From this, the amount of air in the system was calculated. Samples were drawn from the two vents at the top of the tubing and from the fan housing. Unfortunately, it was not possible to completely eliminate the air from the system. The purest fluid obtained had 3% oxygen in it, which corresponded to 14% air. To compensate for this, the properties of the mixed fluid and the associated scaling values were calculated and used for the experiments, as described in chapter 4.

The power scale had to be reduced so that the actual power outputs in the model were larger than they would have been with pure refrigerant. The temperature scale also had to be reduced so that the temperature differences inside the box were larger than they would have been with pure refrigerant. There was added uncertainty in all the properties of the refrigerant and the scaling factors. It was difficult to estimate exactly how much cooling

was being provided at the time of running the experiments, because of these changes, so it was harder to estimate when steady state had been reached.

11.4 Recommendations

It is strongly recommended that only a leak tight box is used for small scale models in future. Ideally, the box would be able to withstand a partial vacuum, so that most of the air could be removed before the box was filled with refrigerant. It could be made out of steel, welded at the joints or possibly out of plexiglass, glued at the joints. If steel were used, it would be difficult to thermally isolate the walls from each other for simulating a hot or cold window. With plexiglass, conduction from heating of cooling coils on the walls would be reduced. Any penetrations should be well sealed. For small holes, Swagelock fittings could be used. The ceiling and the floor should have fittings that could be used for oxygen monitoring, temperature measurement or smoke injection, to provide some flexibility when experiments are run. Space for thicker insulation should be left. Rigid insulation would be easier to install than the flexible type. If a new box were built, it should also have a greater height, so that alternative cheaper, readily available and more environmentally friendly refrigerants could be used, such as R134a, with a temperature scale of one.

12. Uncertainty levels

The uncertainty of all the measurements and some calculated quantities are estimated in table 12.1. The uncertainty of the temperatures read by the thermocouples inside the model decreased when the temperatures were scaled. This did not apply to the gas and water temperature readings, because they were used to calculate the actual cooling provided. Measuring the temperatures at the surface of the water pipes led to a rather large error in the readings, such that sometimes the return temperature was lower than the supply temperature. This may have been because thermal contact was better on the return pipe than the supply pipe. The temperature difference was sometimes as low as 0.4°C so the error was up to 200%. The temperature readings for the cooled ceiling water were much more consistent and the temperature difference was much larger, so the error was only 10%. The cooling provided by the gas was also more reliable, with an error of 10%.

Table 12.1 Uncertainty levels of measured and calculated quantities

Quantity	Instrument / calculation	Source of uncertainty	Magnitude of uncertainty
Space temperatures	Type T thermocouple, DAS 16G, EXP16	Calibration Temperature scale	± 0.5°C measured ± 0.15°C scaled
Internal surface temperatures	Type T thermocouple, DAS 16G, EXP16	Calibration Temperature scale	± 0.5°C measured ± 0.15°C scaled
External wall temperatures	Type T thermocouple, DAS 16G, EXP16	Calibration Temperature scale	± 0.5°C measured ± 0.15°C scaled
Water temperatures	Type T thermocouple, DAS 16G, EXP16	Calibration Conduction through PVC pipe	± 0.8°C
Heat exchanger water temperature difference	Type T thermocouple, DAS 16G, EXP16	Calibration Conduction through PVC pipe	± 200%
Cooled ceiling water temperature difference	Type T thermocouple, DAS 16G, EXP16	Calibration Conduction through PVC pipe	± 10%
Gas temperatures	Type T thermocouple, DAS 16G, EXP16	Calibration	± 0.3°C measured ± 0.1°C scaled
Gas temperatures difference	Type T thermocouple, DAS 16G, EXP16	Calibration	± 7% measured
Height of space thermocouples	Ruler	Movement of thermocouple bead Height of rake above floor	± 3 mm measured ± 20 mm scaled

Table 12.1 Uncertainty levels of measured and calculated quantities (continued)

Quantity	Instrument / calculation	Source of uncertainty	Magnitude of uncertainty
Heater voltages	AC voltmeter	Voltmeter accuracy	± 0.5%
Heater resistances	Ohmmeter	Ohmmeter accuracy	± 0.5%
Heater power outputs	$\frac{(\text{Voltage})^2}{\text{Resistance}}$	Voltage, resistance R114 purity, power scale	± 1%
Heat exchanger water flow rate	Rotameter	Calibration	± 2.5%
Cooled ceiling water flow rate	Rotameter	Calibration	± 5%
Heat exchanger water cooling	Density x flow rate x specific heat x temp. difference	Water temperature measurement	± 200%
Cooled ceiling water cooling	Density x flow rate x specific heat x temp. difference	Water temperature measurement	± 20%
R114 purity	Fyrite II analyzer	Calibration	± 2.5% of R114 concentration
Gas flow rate	Heat exchanger calibration	Extrapolation R114 purity	± 4%
Gas cooling	Density x flow rate x specific heat x temperature difference	Gas flow rate calibration R114 purity Heat gains	10%
Stratified layer thickness	Observation of smoke	Observation	± 10 mm measured ± 0.07 m scaled

13. Experiments

13.1 Description

The first set of experiments carried out was on displacement ventilation alone. The heat loads of the electrical resistances were nominally for full scale loads of 20, 30, 40, 60 and 80 W/m^2. However, the amount of air in the system varied for each experiment and affected the scaling factors, particularly for the temperature and the power. The actual heat loads were calculated to be between 9 and 48 W/m^2, found from the heat gained by the gas in the space, q_g, which equalled the cooling provided by the gas. The calculation used the gas flow rate, Q_g, the temperature difference between the diffuser temperature, T_d, and the average of the temperatures of the highest two thermocouples on the rake, T_t.

Cooling by gas in space, $\quad q_g = \rho_g \, Q_g \, c_{p\,g} \, (T_t - T_d)$

These cooling loads are used in the results. A summary of the experimental conditions is given in table 13.1.

The gas was supplied at a design temperature of 19 °C and the temperatures were scaled using a reference temperature of 19 °C. This temperature was controlled by adjusting the water flow rate manually. Readings were taken using the data acquisition system once the temperatures appeared to be steady. It took one set of readings each time the program, THERM4.BAS, was run. The rake was moved along the length of the box and seven sets of readings were taken.

The oxygen concentration was measured for each experiment and used to adjust the properties of the refrigerant and the scaling factors. The percentage of supply voltage provided across each resistor was noted, as was the flow rate of water through the heat exchanger and the pressure drop read by the manometer across the gas side of the heat exchanger, which indicated the gas flow rate. The electrical power supplied was calculated from the voltage, V, and the resistance, R, as shown in table 7.2. It equalled the electric heat loads in the space. The cooling provided by the water, q_{wHE}, was found from the water flow rate through the heat exchanger, Q_{wHE}, and the difference between the supply water temperature, T_{ws}, and the return water temperature, T_{wr}. The total cooling provided by the gas, q_g, was found from the gas flow rate, Q_g, and the difference between the supply and the return water temperatures.

Electric heat loads, $\quad q_e = V^2/R$ for each resistor

Cooling by water $\quad q_{wHE} = \rho_w \, Q_w \, c_{p\,w} \, (T_{wr} - T_{ws})$

Total cooling by gas $\quad q_{gHE} = \rho_g \, Q_{gHE} \, c_{p\,g} \, (T_{gr} - T_{gs})$

If the box and the gas and water system had been perfectly insulated and steady state had been reached, then the electrical power, the cooling provided by the water and the total cooling provided by the gas should all have been the same. However, this was not the case. The gas extract or return temperature was consistently much lower than the gas temperature at the top of the thermocouple rake and the gas supply temperature was consistently a little lower than the gas temperature at the diffuser. Therefore, there must have been heat transfer through the gas tubing walls, which were not insulated. The

surface temperature of the side false wall was always less than the space temperatures at the same height, so there was probably some heat transfer through the false wall where the gas was supplied and there may have been some short circuiting of the supply gas through the small gaps at the sides of the false ceiling. The surface temperatures of the side and end outside walls were also less than the space temperatures at the same height, so there was heat loss to the outside also. Therefore the insulation on each of these walls should have been better. The only wall that was adiabatic, was the false wall at the end. This was because there was a 14 cm gap between this wall and the outside wall and the gas in the gap was still, acting as an insulating later.

The temperature readings of the water supply to and return from the heat exchanger had errors of ± 0.8 °C, and the error in the difference between them was ± 200%, as described in chapter 12. Therefore, the calculated cooling provided by the water was very unreliable and was not used in the analysis of the results.

It was difficult to reach steady state because the gas could only be kept at a constant concentration for a relatively short time, about an hour for each experiment. When the results were analyzed, it was found that a much longer time would have been needed, perhaps three hours. At the time of the experiments, the MIT supply water temperature was rather high, at around 13 °C, instead of the design of 6.1 °C, so the mean temperature difference between the gas and the water in the heat exchanger was small and the amount of cooling that could be provided was limited. For electric heat loads of greater than 60 W/m^2, it is probable that there was insufficient cooling capacity on the water side to keep the temperatures close to room temperature, which would make the scaled temperatures realistic and comfortable using a reference temperature of 19 °C. Steady state could only have been attained at much higher temperatures. Then the temperatures would have had to have been scaled using a lower reference temperature. As the temperatures in the box were 10 to 40 K higher than room temperature, the heat losses from the box were also high.

Two sets of experiments were carried out with the chilled ceiling, one with a supply rate of approximately 7.8 air changes per hour and the next with approximately 18.3 air changes. See table 13.1. When the cooled ceiling was used, the flow rate through the cooled ceiling pipework, Q_c was also noted. The cooling provided by the ceiling, $q_{w\,c}$, was found from the water flow rate through the ceiling panel, Q_c, and the difference between the supply water temperature to the ceiling panel, T_{cs}, and the return water temperature, T_{cr}.

Table 13.1 also shows the ventilation cooling and the convective cooling. The total cooling provided to the space was the sum of the ceiling cooling and the ventilation cooling. The ventilation cooling provided by the gas, q_v, was found from the gas flow rate, Q_g, and the difference between the temperature at the ceiling, T_c, and the diffuser temperature, T_d. The thermocouples measuring the temperature at the ceiling were designed to measure the surface temperature. Thermal paste was used to make a good thermal connection. However, the temperatures measured show that they were measuring the gas temperature close to the ceiling. Both thermocouples were located close to the extract grilles, so it was assumed that they were reading the temperature of the extract gas. The convective part of the cooling provided by the ceiling, $q_{c.conv}$, was found from the gas flow rate, Q_g, and the difference between the temperature at the top of the thermocouple rake, T_t, and the temperature at the ceiling, T_c. The combined convective cooling, q_g , was found in the same way as for displacement ventilation alone. The results were characterized using this cooling amount.

Ceiling cooling $$q_c = \rho_w Q_{w\,c} c_{p\,w} (T_{cr} - T_{cs})$$

Ventilation cooling $q_v = \rho_g Q_g c_{p\,g} (T_c - T_d)$

Convective cooling by ceiling $q_{c.conv} = \rho_g Q_g c_{p\,g} (T_t - T_c)$

Combined convective cooling $q_g = \rho_g Q_g c_{p\,g} (T_t - T_d)$

$q_g = q_v + q_{c.conv}$

Radiative cooling by ceiling $q_{c.rad} = q_c - q_{c.conv}$

Total cooling $q_t = q_c + q_v$

The calculated total cooling was significantly higher than the electric heat loads for each case, even allowing for errors of up to 25%. This could have been because steady state was not reached and the apparatus had stored some heat from previous experiments as it had some capacitance, particularly for experiments 34 to 36, when the heat loads were decreased. Olson[6] calculated that the thermal capacitance of the apparatus was 87.4 kJ/K (Appendix B, page 232), so for a rate of change of temperature of 1 K/hr, the energy storage would be 24 W or 32 W/m^2. The analysis assumes that the effective heat load in the space was equal to the total cooling provided at a quasi steady state, i.e. when the temperature profile was near constant.

13.2 Displacement ventilation results

A summary of the results is given in table 13.1. The temperatures are the average of all the readings, for the seven sets and the two columns. They have been shifted so that they correspond to a supply temperature of 19°C, if it was not exactly that in the experiment, to facilitate comparison of the results. Figure 13.1 shows the temperature results for three experiments, numbers 14, 2 and 30, at cooling loads of 9, 18 and 25 W/m^2 respectively. They had a full scale supply air flow rate of about 7.5 air changes per hour (ac/h) which produced a supply air velocity of 0.15 m/s. They show a fairly vertical temperature gradient up to about 1.1 m in height and then a rise in temperature of between 1 and 3 K. The rise is greatest for the load of 25 W/m^2, but it is within Svensson's[7] stringent comfort level of 3 K between 0.1 m and 1.8 m. The supply velocity is on the comfort limit of 15% people dissatisfied with 0.15 m/s at 20°C, for someone standing in front of the diffuser.

Figure 13.2 shows the temperature distribution for displacement ventilation with an air change rate of about 13. The experiment numbers were 5, 8 and 11, at cooling loads of 30, 35 and 48 W/m^2 respectively. The temperature gradient were similar in shape to the lower flow rate cases. The temperature differences were slightly higher, with between 0.4 and 2 K up to 1.1 m and a maximum difference of 4 K over the whole height for 48 W/m^2. These temperature gradients are acceptable for thermal comfort, but the supply air velocity is rather high for comfort, at 0.26 m/s. For these conditions, the use of the space would be restricted, because no desks could be put near the diffusers.

The temperatures near the floor remained quite close to the supply air temperature measured at the diffuser. This is different from results of investigations into displacement ventilation by Elisabeth Mundt[15], which show that the air is heated by 1 or 2 K as it moves across the floor, before it reaches any heat sources. This difference is probably due to reduced radiation exchange between the warm ceiling and the cool floor, because the refrigerant absorbs about 63% of radiation energy emitted from a surface.

Table 13.1 Summary of results

Displacement ventilation alone

Experiment number	1	2	5	8	11	14	17	21
Electric heat loads, W/m^2	14	26	19	26	38	9	27	28
Cooling, W/m^2	18	18	30	35	48	9	17	28
Supply flow rate, l/s m^2	7.4	5.9	9.3	9.8	9.8	5.3	7.2	9.9
Air changes per hour	9.8	7.8	12.3	12.9	12.9	6.9	9.5	13.1
Supply velocity, m/s	0.19	0.16	0.24	0.26	0.26	0.14	0.19	0.26
Heights, m	Temperatures, degrees C							
2.4	20.9	21.6	21.8	22.0	23.1	20.3	20.9	21.7
2	20.6	21.4	21.1	21.9	22.8	20.0	20.5	21.4
1.7	20.4	21.0	20.5	21.5	22.4	19.8	20.3	21.2
1.1	19.6	19.8	19.6	20.1	21.1	19.4	19.6	20.4
0.85	19.3	19.5	19.5	19.6	20.3	19.3	19.4	20.0
0.6	19.2	19.3	19.4	19.4	19.7	19.2	19.3	19.7
0.3	19.1	19.2	19.3	19.3	19.5	19.2	19.2	19.4
0.1	19.1	19.2	19.3	19.2	19.4	19.2	19.2	19.3

With cooled ceiling

Experiment number	30	31	32	33	34	35	36
Electric heat loads, W/m^2	18	36	56	79	79	58	31
Ceiling cooling, W/m^2	0	31±4	49±15	78±23	83±25	69±20	32±9
Ventilation cooling, W/m^2	25±3	27±3	28±3	40±4	74±8	52±5	41±4
Convective cooling, W/m^2	25±3	40±4	40±4	60±6	105±11	70±7	55±6
Ceiling convective cooling	0	13	12	20	31	18	14
Ceiling radiative cooling	0	18	37	58	52	51	22
Total cooling, W/m^2	25	58	77	118	157	121	73
% ceiling cool. by radiation	-	58	76	74	63	74	69
% cooling by ventilation	100	47	36	34	47	43	56
Supply flow rate, l/s m^2	5.8	5.9	5.9	5.9	13.5	14.1	14.0
Air changes per hour	7.7	7.8	7.8	7.8	17.9	18.6	18.4
Supply velocity, m/s	0.15	0.16	0.16	0.16	0.36	0.37	0.37
Heights, m	Temperatures, degrees C						
2.4	22.6	24.7	24.9	27.5	26.0	23.5	22.5
2	22.4	24.5	24.8	27.4	25.8	23.3	22.4
1.7	22.0	24.2	24.6	27.2	25.5	23.1	22.2
1.1	20.0	22.3	22.6	25.6	23.6	21.3	20.8
0.85	19.5	20.0	20.4	23.5	21.4	20.4	20.1
0.6	19.3	19.4	19.6	20.9	20.3	19.9	19.7
0.3	19.1	19.1	19.2	19.7	19.6	19.5	19.4
0.1	19.1	19.0	19.1	19.2	19.3	19.3	19.3

Figure 13.1 Displacement ventilation, 7.5 ac/h

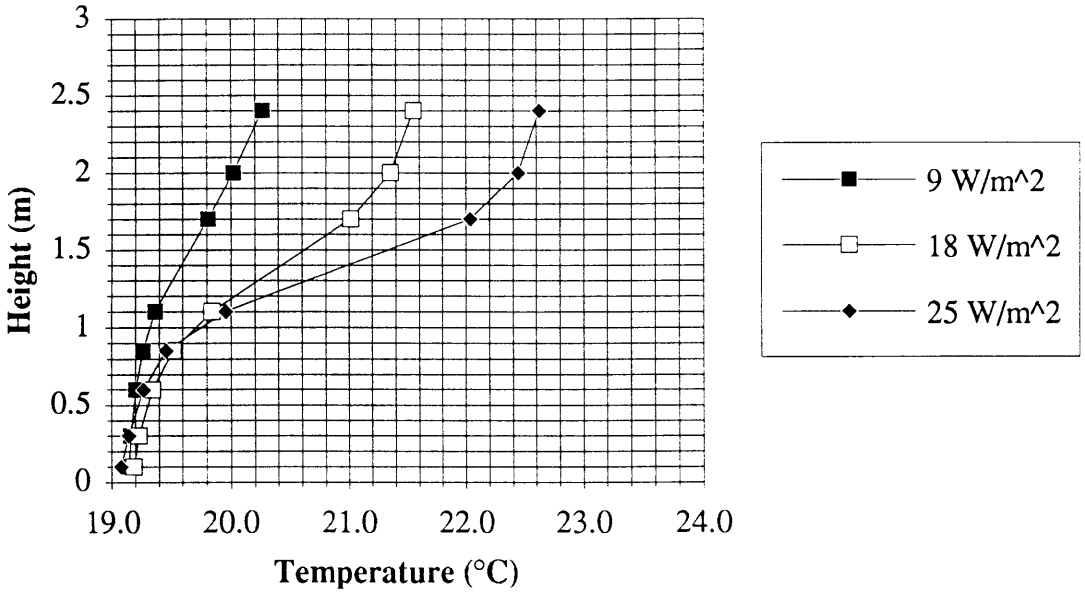

Figure 13.2 Displacement ventilation, 13 ac/h

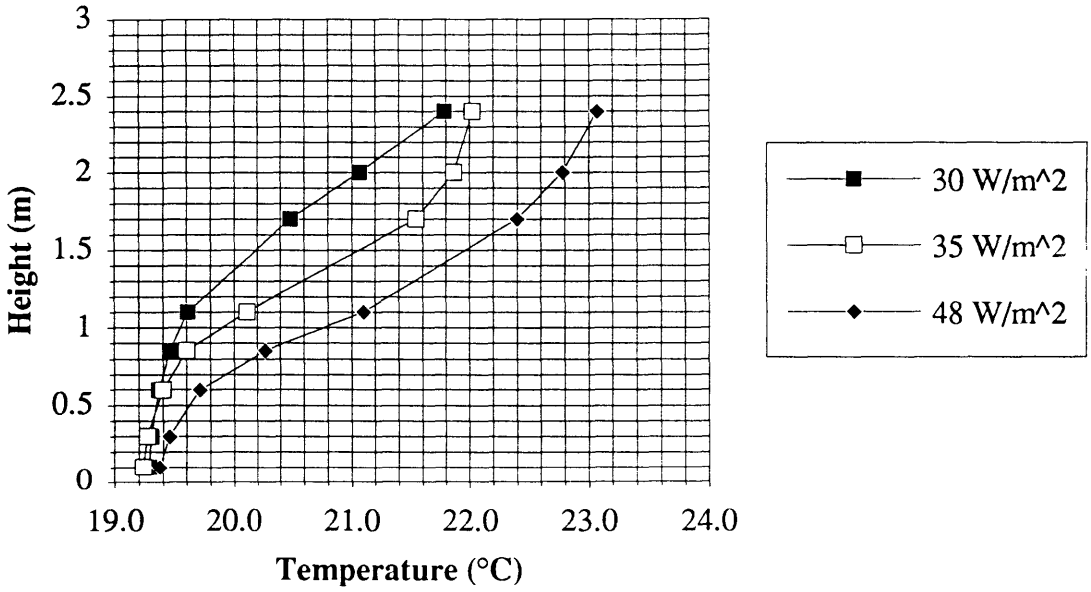

13.3 Displacement ventilation flow visualization

The flow dropped down from the diffuser in the characteristic displacement ventilation pattern. It then flowed across the floor and plumes could be seen rising around the standing people and from the computers. Some gas flowed back horizontally in the direction of the diffuser at high level. It was probably being displaced from the top of the plume from the cylinder representing a person standing, as there were no other heat sources in that area. No stationary layer at high level could be seen. The supply air rate was relatively high for a displacement system. If it were higher than the rate of flow due to natural convection and buoyancy around the heat sources, then the hot gas would have been extracted as soon as it reached the ceiling, hence no stationary layer would be seen. This means that the air quality was close to that of the supply air around the heat sources, which is much better than for a mixed system.

The flow visualization could be improved by adding ports to the ceiling so that smoke could be injected at points of interest inside the model room, such as directly above or at the side of a heat source and at the diffuser. Care would have to be taken that the smoke was injected at very low velocity, so that it wouldn't affect the room flows. Injecting the smoke into the supply behind the false side wall ensured that the smoke didn't alter the flow patterns, but it meant that once the smoke dispersed in the room, it was difficult to see the flow patterns unless they were very significant.

13.4 Displacement ventilation with cooled ceiling results

Figure 13.3 shows the profiles for cases with a supply air rate of about 7.8 ac/h. These were experiment numbers 30 to 33, at total cooling loads of 25 to 118 W/m^2. The temperature profiles with the cooled ceiling were similar in shape to those for displacement ventilation alone, although they made more distinctive S-shaped curves. The gradient was steeper at the lower level, below 0.85 m. Then it flattened out from around 0.85 m to 1.7 m and became close to vertical above 2m. Much higher loads could be cooled than by displacement ventilation alone for the same supply air rate. The 25 W/m^2 case does not have any cooling from the ceiling. The comfort limit of 3 K between 0.1 and 1.1 m is reached at a cooling load of 77 W/m^2. Experiments 31 and 32 have very similar temperature profiles, but different cooling loads, which is accounted for by different radiative cooling by the ceiling. Therefore, as the heat load increased and the gas supply rate remained constant, the surface temperatures of the heat sources increased, so the amount of radiation to the ceiling increased. The temperatures rise steeply at around the 1.1 m height and then become almost vertical above 2 m. This suggests that there is still some displacement at low to mid level, particularly for the lower heat loads, but at high level, above 2 m, the flow is mixed.

Results for a greater air change rate of approximately 18.3 are shown in figure 13.4. These were for experiment numbers 34, 35 and 36, at cooling loads of 73, 121 and 157 W/m^2. The temperature gradients are acceptable up to 121 W/m^2 but the supply air velocity of 0.37 m/s would create a large uncomfortable zone in front of the diffuser. Comparing the 73 W/m^2 case at 18.3 ac/h with the 77 W/m^2 case at 7.8 ac/h, the temperature gradient is much more vertical with the higher flow rate, up to 1.1 m. This is probably because the supply volume is large and is not affected much by heat gains until it reaches a higher level. At the lower flow rate, the temperatures are more sensitive to the heat gains at low level.

The estimated proportion of cooling by the displacement ventilation was between 36% and 56%. The cooling by displacement ventilation is significant, so it can be expected that the

buoyant air flow characteristic is still present, and the ceiling adds to the cooling provided. The proportion of the ceiling cooling that was by radiation was between 58% and 76%. The error in these estimates is up to 25%.

The maximum cooling load found from this study with a supply velocity below the comfort level of 0.25 m/s at 19°C is 77 W/m^2. In this case, the ventilation provided about 36% of the cooling. However, the effects of radiation are not modelled completely, because refrigerant R114 absorbs about 63% of radiation at 300 K. Kulpmann showed in full scale tests that there was a temperature change of 2 K between 0.1 m and 0.7 m for a cooling load of 50 W/m^2, where the ventilation contributed 25% of the cooling and the supply air rate was 3.2 air changes per hour. With a cooled ceiling alone, the temperature gradient was almost vertical.

The cooling load in this study was limited by the supply water temperature from the MIT system. The supply to the ceiling was approximately 15.5°C in reality which scaled to 18°C. The average ceiling water temperature could have been reduced to 16°C which would correspond to a supply water of 7.5°C. The temperatures measured at the ceiling were between the highest temperature measured on the rake and the extract temperature, so it is suspected that these were air temperatures rather than surface temperatures. Therefore the maximum cooling load in this study could be increased by lowering the ceiling surface temperature and by using a gas which is less radiatively absorbing at these temperatures. The radiation cooling effect of the ceiling could be checked by running an experiment with no ventilation at all or just enough to satisfy minimum outdoor air requirements. That would be 8 l/s/person i.e., 24 l/s for the room and 1 air change per hour. Then, all or almost all the convection cooling measured by the change in temperature of the gas from supply to extract would be provided by the ceiling, and the remainder of the ceiling cooling would be by radiation. Another way to check the effect of radiation would be to measure the surface temperatures of all the heat sources, as well as of the ceiling, floor and walls. If the emissivities of the surfaces and the absorptance of the gas were known, then the cooling by radiation from the ceiling could be calculated independently.

13.5 Displacement ventilation with cooled ceiling flow visualization

For heat loads of up to 58 W/m^2 the flow patterns seemed to be similar to those with displacement ventilation alone. See figure 13.5. A layer of gas built up at low level up to about the height of diffuser, 0.78 m in full scale. No plumes could be seen, but another layer of gas built up at high level, down to about the top of the person sitting down, 1.1 m, and some flow was seen returning horizontally in the direction of the diffuser. There was a clear thin layer in between. The bottom layer fluctuated up and down. At higher loads, no special flow patterns could be seen, and the smoke appeared to be mixed. This suggests that displacement flow occurred at low level, below the breathing zone, but at higher levels, above 1.1 m, the convection cooling from the cooled ceiling dominated and disturbed the displacement flow. The air quality is probably better than for a mixed system for someone sitting down, but just the same for someone standing up.

13.6 Comparison of displacement ventilation with and without a cooled ceiling

Figure 13.6 shows a comparison of experiments with and without a cooled ceiling. The shapes of the temperature profiles do not appear to be significantly different. The product of the temperature difference between the top and the bottom of the profile and the flow rate gives an indication of the convection cooling. For displacement ventilation, this is the total

cooling. For the cases with the cooled ceiling, the radiative component of the ceiling adds to the cooling provided, so for the same comfort condition in terms of the profile and supply velocity, the ceiling provides more cooling than displacement ventilation alone. It may also improve the comfort by cooling the occupants' heads radiatively and decreasing the mean radiant temperature.

Figure 13.3 Displacement ventilation with cooled ceiling, 7.8 ac/h

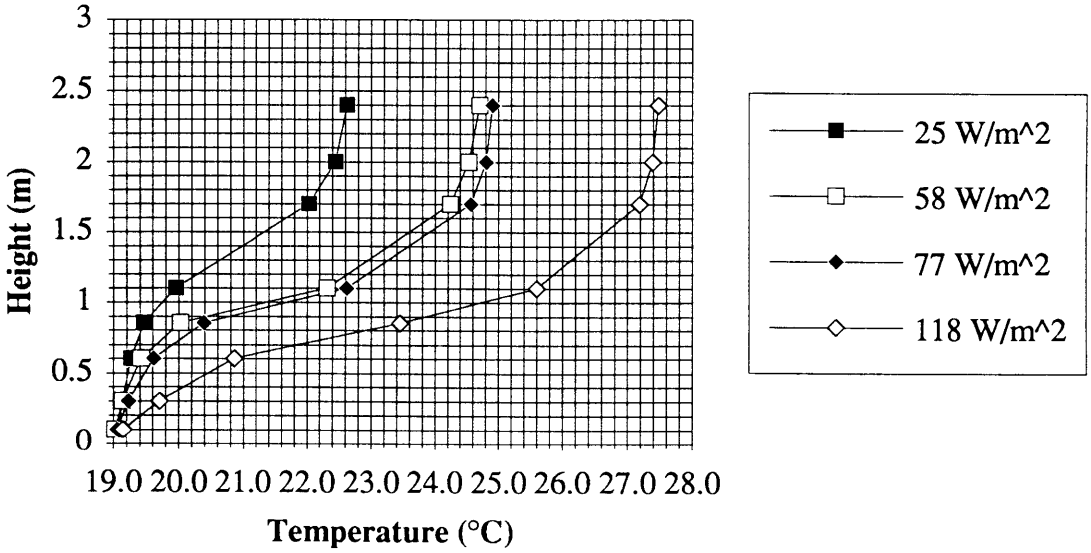

Figure 13.4 Displacement ventilation with cooled ceiling, 18.3 ac/h

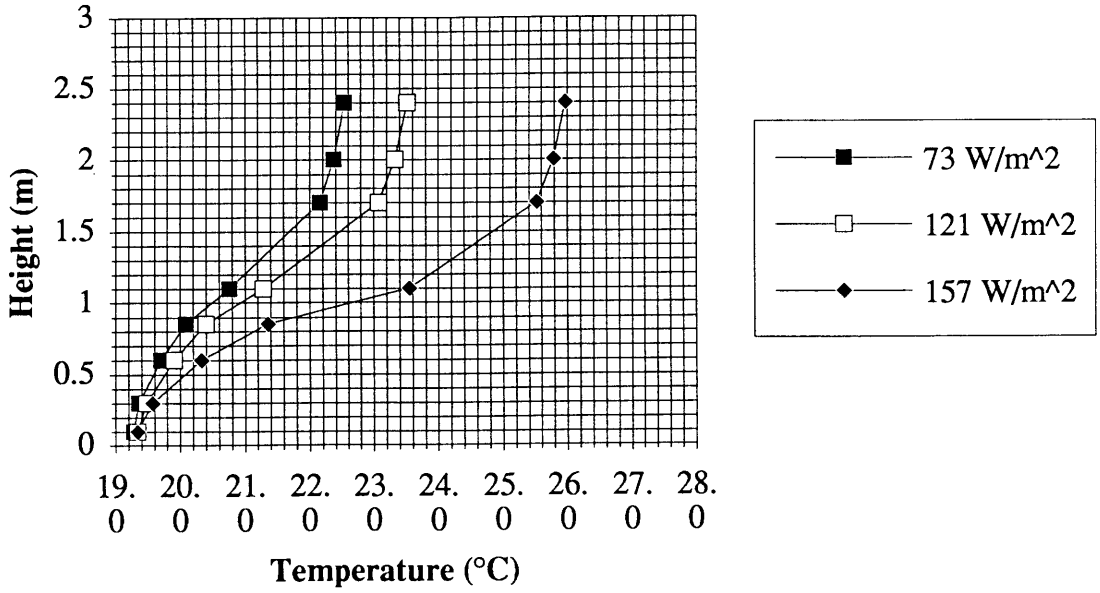

Figure 13.5 Photo of flow visualization for displacement ventilation with a cooled ceiling

Experiment number 31, cooling 58 W/m^2

Figure 13.6 Comparison of displacement ventilation with and without a cooled ceiling

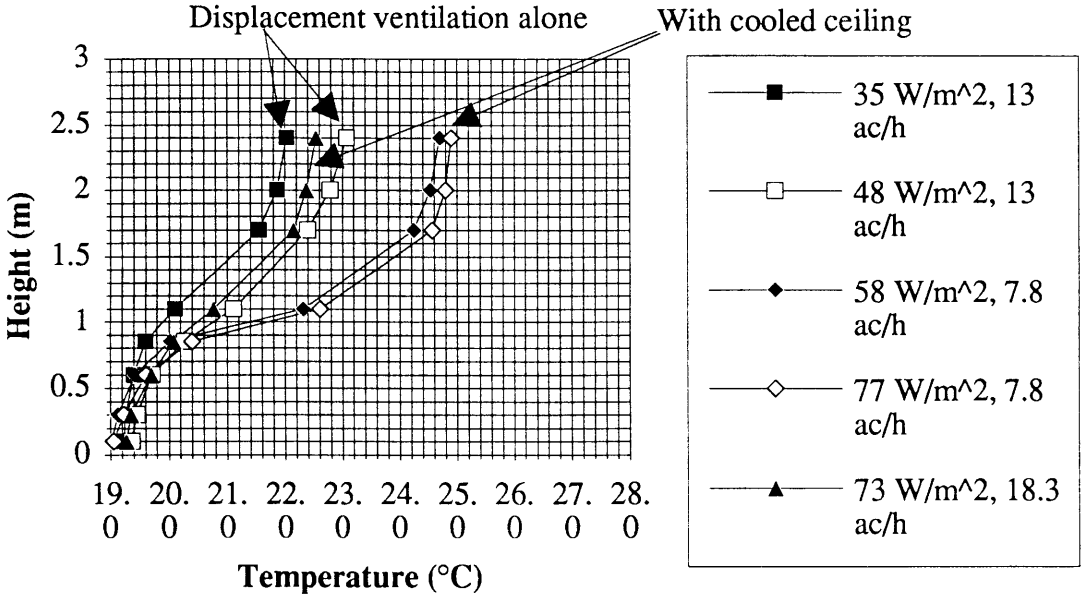

14. Conclusions

14.1 Displacement ventilation

Displacement ventilation can be comfortable for heat loads of at least 25 W/m^2 with an air change rate of 7.5 and a supply air velocity of 0.15 m/s, using the stringent limit of 3 K between 0.1 m and 1.8 m. The temperature difference between the ankle and head heights of someone sitting down, 0.1 and 1.1 m, would be approximately 1.6 K at this condition. It is estimated that the less specific comfort limit of 3 K between 0.1 and 1.1 m would be reached when the heat loads rose to 45 W/m^2. If a higher supply air velocity of 0.26 m/s could be tolerated, the temperature gradient would remain comfortable for heat loads of at least 48 W/m^2.

14.2 Displacement ventilation with a cooled ceiling

Larger heat loads could be cooled whilst keeping the same temperature gradient with the addition of a cooled ceiling, compared with displacement ventilation alone. The gradient depends on the supply rate of the air and the convective cooling by the ceiling, for a given heat load. The temperature gradient of the space is comfortable for loads of up to 77 W/m^2 for 7.8 air changes per hour and a supply velocity of 0.16 m/s and up to 121 W/m^2 for 18.3 air changes per hour and a supply velocity of 0.37 m/s. However, this velocity is larger than the comfort limit of 0.25 m/s at 19°C. The amount of cooling by radiation from the ceiling was between about 58% and 76% of the ceiling cooling. This study was conservative on the influence of radiation cooling, because the refrigerant absorbed about 63% of the radiation emitted from the ceiling. A full scale study with air should show more influence. Also, the ceiling surface temperature was probably higher than the minimum temperature of 16 °C, because of heat gains along the water pipes and the high supply temperature of the MIT water system. The maximum cooling load in this study for comfortable conditions was 77 W/m^2. This load could be increased by using a gas which is less radiatively absorbing and by lowering the ceiling surface temperature.

14.3 Air quality

Flow visualization shows that the enhanced air quality associated with displacement ventilation is partly maintained with the addition of a cooled ceiling for loads of up to about 58 W/m^2 with 7.8 air changes per hour, where displacement ventilation accounts for about 47% of the cooling provided. The supply gas reached a level of about 1.1m, which is the height of the breathing zone for someone sitting down. Above 1.1m, there was some mixing of the gas from higher up, which would be contaminated by emissions from the heat loads and materials in the room. At higher loads, the displacement effect is not seen, although there are still significant temperature gradients. This is probably because the gas at the ceiling is cooled enough to make it drop down below the stationary layer into the occupied region, to a height of about 1.1 m. It would then be heated by the heat sources and rise up again. It is not clear if the air quality was any better than for a mixed system for loads of greater than 58 W/m^2.

14.4 Recommended use of cooled ceilings

Cooled ceilings can be used to increase the cooling provided to a space in conjunction with displacement ventilation. Some improved air quality can be maintained for people sitting

down for loads of up to 58 W/m^2. They can be used in addition to a displacement ventilation system to increase the cooling above 58 W/m^2 when necessary, but the enhanced air quality would then probably be lost. For higher loads, the supply air rate can be reduced to keep the temperature gradient comfortable. When the loads are lower than 45 W/m^2, or 25 W/m^2 for greater comfort, the displacement ventilation can work alone and provide good air quality for the occupants.

14.5 Further study

The interaction of cooled ceilings with displacement ventilation could be studied in more detail by varying the supply rate of air, including conducting one test with the minimum outside air rate of 1 air change per hour. The effect of the cooled ceiling could be checked by using it with no ventilation at all. Suggestions for improving the experimental procedure are given below. Tests could be run at the same heat load whilst varying the ventilation rate. The comparison of comfort with displacement ventilation with and without the cooled ceiling would be facilitated by running tests at the same supply air rates and different heat loads.

14.6 Future use of small scale modelling

The use of a small scale model with refrigerant enabled the study of temperatures and flow patterns within a space without having to build a full scale model. However, the radiative absorption characteristic of the refrigerant meant that the results of this study were not complete. If a small model is continued to be used, it is recommended that a different refrigerant be used, which is more friendly to the environment, cheaper, more readily available and less radiatively absorbing. R134a fits the first three criteria. Its absorptance would have to be found out or measured to determine whether it would be suitable or not.

A leak tight box with a greater height should be built, to avoid wasting refrigerant and harming the environment and so that experiments can be run over several days and weeks, to be sure that steady state is reached and so that results can be checked. This would also reduce the amount of air mixed in with the refrigerant and the resulting uncertainties in the refrigerant properties and scaling factors. If a larger box were used, a refrigerant with a smaller scaling factor could be used, such as R134a, which is an HCFC and is more friendly to the environment and so that a temperature scale of one can be used. This would make analysis of the results easier, but the advantage of reducing the error in the temperature readings would be lost.

The temperature measurements of the water could be improved by inserting the thermocouples into sealed holes in the pipe, like the gas measurements. Also the insulation could be more extensive on all the piping and tubing, as well as around the box and at the false walls, to reduce heat losses or gains. Any gaps at the edges of the false walls or ceiling should be closed to prevent the gas from short circuiting. It is recommended that the temperature of the extract gas be measured at the extract grille and the temperatures of the supply and return water for the cooled ceiling be measured as close as possible to the ceiling. The thermocouples measuring the temperature of the ceiling surface should be more firmly attached. The temperature of the primary water supply should be closer to the design temperature of 6.1 °C to provide a greater cooling capacity and controllability. The flow measurement of the gas could be improved by calibrating the flow through an orifice plate, where the pressure drop across it can be modelled more accurately.

Reference List

Cited references

1. ISO 1984, International Standard 7730, "Moderate thermal environments - determination of the PMV and PPD indices and specification of the conditions for thermal comfort", Geneva: International Standards Organization.

2. ASHRAE 1981, ASHRAE Standard 55-1981, "Thermal environmental conditions for human occupancy" Atlanta: American Society of Heating, Refrigerating and Air-Conditioning Engineer, Inc..

3. B.W. Olesen, M. Scholer and P.O. Fanger, 1979, "Discomfort caused by vertical temperature differences" in: P.O. Fanger and O. Valbjorn (eds.), Indoor Climate, Danish Building Research Institute, Copenhagen, pp. 561 - 579.

4. D.S. Fishman and A. Semere, 1977, "A preliminary investigation into the subjective effects of low-level draughts (temperature variation)", British Gas Corporation Report WH/T/R&D/77/12, London.

5. D.S. Fishman and S.E. Underwood, 1977, "A further investigation into the subjective effects of low-level draughts (temperature and velocity variation)", British Gas Corporation Report WH/T/R&D/77/145, London.

6. Douglas Olson, September 1986, "Scale model studies of natural convection in enclosures at high Rayleigh number", PhD. thesis, Massachusetts Institute of Technology.

7. A.G.L. Svensson, 1989, "Nordic experiences of displacement ventilation systems", ASHRAE Transactions 95(2), pp.1013-1017.

8. M. Sandberg and C. Blomqvist, 1989, "Displacement ventilation systems in office rooms", ASHRAE Transactions 95(2), pp.1041-1049.

9. O.A. Seppanen, W.J. Fisk, J. Eto, and D.T. Grimsrud, "Comparison of conventional mixing and displacement air-conditioning and ventilation systems in U.S. commercial buildings", ASHRAE Transactions 95(2), pp.1028-1040.

10. M. Mattsson and M. Sandberg, 1994, "Displacement ventilation - influence of physical activity", Proceedings, Roomvent '94, Poland, Volume 2.

11. R.W. Kulpmann, 1993, "Thermal comfort and air quality in rooms with cooled ceilings - results of scientific investigations", ASHRAE Transactions 99(2).

12. R. Siegel and J.R. Howell, 1972, " Thermal Radiation Heat Transfer", McGraw-Hill, Inc.

13. Mehmet Okutan, 1995, "Displacement ventilation", Masters thesis, MIT.

14. Frank Revi, February 1992, "Measurement of two-dimensional concentration fields of a glycol-based tracer aerosol using laser light sheet illumination and microcomputer video image acquisition and processing", M.S. thesis, Massachusetts Institute of Technology.

15. E. Mundt, "Convection flows above common heat sources in room with displacement ventilation", Proceedings Room Vent '90, Oslo, Norway, June 13-15, 1990.

Other references

Displacement ventilation

ASHRAE 1993 Fundamentals Handbook, "Displacement Ventilation", chapter 31, pp.31.4-31.5.

Ove Arup HVAC Applications Guide, October 1993, "Displacement Ventilation", section 7.5, 13 Fitzroy Street, London, W1P 6BQ, England.

Yuguo Li, Laszlo Fuchs and Mats Sandberg, April 1993, "Numerical prediction of airflow and heat-radiation interaction in a room with displacement ventilation", Energy and Buildings, 20(1), pp.27-43.

Mats Sandberg and Mats Sjoberg, "A comparative study of the performance of general ventilation systems in evacuating contaminants", pp.59-64.

Mats Sandberg and Magnus Mattsson, December 1993, "Density currents created by supply from low velocity devices", The National Swedish Institute for Building Research, TN:44.

M. Sandberg and S. Lindstrom, "Stratified flow in ventilated rooms - a model study", Proceedings Room Vent '90, Oslo, Norway, June 13-15, 1990.

P. Heiselberg and M. Sandberg, "Convection from a slender cylinder in a ventilated room", Proceedings Room Vent '90, Oslo, Norway, June 13-15 1990.

M. Sandberg and S. Holmberg, "Spread of supply air from low-velocity air terminals", Proceedings of Room Vent '90, Oslo, Norway, June 13-15, 1990.

C.W.F. Cox, J. Ham, J.M. Koppers and L.L.M. van Schijndel "Displacement Ventilation Systems in Office Rooms - a Field Study", Proceedings Room Vent '90, Oslo, June 1990.

E. Skaret, Ventilation by Displacement - characterization and design implications", Proceedings Ventilation '85 (ed H.Goodfellow), Toronto, Canada, Elsevier Science Publishers.

Yuguo Li, Mats Sandberg and Laszlo Fuchs, September 25 1992, "Effects of thermal radiation on airflow with displacement ventilation: an experimental investigation", Energy and Buildings, 19(4), pp.263-274.

H.M. Mathisen, 1989, "Case studies of displacement ventilation in public halls", ASHRAE Transactions, 95(2), pp.1018-1027.

A.K. Melikov and J.B. Nielsen, 1989, "Local thermal discomfort due to draft and vertical temperature difference in rooms with displacement ventilation", ASHRAE Transactions 95(2), pp.1050-1057.

Lars Davidson and Erik Olsson, September 1989, "Ventilation by displacement: calculation of the flow in a three-dimensional room", 10th AIVC conference, Dipoli, Finland, Paper 20, pp.367-391.

B. Kegel and U.W. Schulz, September 1989, "Displacement ventilation for office buildings", 10th AIVC Conference, Dipoli, Finland, Paper 21, pp.392-411.

Peter V. Nielsen, Lars Hoff, Lars Germann Pedersen, September 1988, "Displacement ventilation by different types of diffusers", 9th AIVC Conference, Gent, Belgium, Poster 2.

Derek J. Croome, September 1988, "A comparison of upward and downward air distribution systems", 9th AIVC Conference, Gent, Belgium, Poster 3.

Hans Martin Mathisen, September 1988, "Air motion in the vicinity of air-supply devices for displacement ventilation", 9th AIVC Conference, Gent, Belgium, Paper 7.

N.O. Breum and J. Skotte, October 1992, "Displacement ventilation in industry - a design principle for improved air quality", Building and Environment, 27(4), pp.447-453.

Qingyan Chen and Jan van der Kooi, 1990, "A methodology for indoor airflow computations and energy analysis for a displacement ventilation system", Energy and Buildings, 14(4), pp.259-271.

D.P. Wyon and M. Sandberg, 1990, "Thermal manikin prediction of discomfort due to displacement ventilation", ASHRAE Transactions, 96(1), pp. 67-75.

Vladimir Prochaska, October 1991, "Optimum control of displacement ventilation", H&V Engineer, 64(709), pp.12-15.

Rob Shackleton, "Learning from the past. Old buildings give lessons in energy efficiency", 1993, H&V Engineer, 66(718), pp.8-9.

Paul Haddlesley, July 1993, "An upward trend", Heating & Air Conditioning, pp.14, 17.

Barrie Evans, November 17 1993, "Low-energy design for a high-tech office", Architects Journal, 198(19), pp.29-32.

Paul Appleby, October 1990, "Researching air movement", Building Services, pp.53-54.

Paul Appleby, April 1989, "Displacement ventilation: a design guide", Building Services, pp.63-66.

H.E. Martin, March 1989, "Ventilating for comfort", Building Services, 11(3), pp.36-37.

Paul Appleby, November 1986, "Low level supply: application and design", Building Services, pp.59 - 62.

Chilled Ceilings

U. Busweiler, 1993, "Air Conditioning with a combination of radiant cooling, displacement ventilation and desiccant cooling", ASHRAE Transactions 99(2).

G. Zweifel, 1993, "Simulation of displacement ventilation and radiant cooling with DOE-2", ASHRAE Transactions 99(2).

M.F. Brunk, 1993, "Cooling ceilings - an opportunity to reduce energy costs by way of radiant cooling", ASHRAE Transactions 99(2).

Christopher K. Wilkins and Risto Kosonen, August 1992, "Cool ceiling system: A European air-conditioning alternative", ASHRAE Journal, pp.41 - 45.

Peter Holdsworth, 11/18 August 1994, "Chilling Stuff", Property Week, pp. 22 - 24.

Paul Appleby, July 1988, "A ceiling for cooling", Building Services, pp.57 - 59.

Barrie Evans, November 3 1993, "The many benefits of a chilled ceiling", Architects Journal, 198 (17), pp.30-33.

Roderic Bunn, November 1991, "The future for cooling ceilings", Building Services, pp.33

Terry Wyatt, November 1991, "Chilled beams and displacement ventilation", Building Services, pp. 34.

Comfort

P.O. Fanger, A.K. Melikov, H. Hanzawa and J. Ring, 1988, "Air turbulence and sensation of draught", Energy and Buildings, 12, pp.21-39.

J.S. Zhang, G.J. Wu, L.L. Christianson, "Full-scale experimental results on the mean and turbulent behavior of room ventilation flows", ASHRAE Transactions, pp.307-318.

J.L.M. Hensen, 1990, "Literature review on thermal comfort in transient conditions", Building & Environment, Vol.25, No. 4, pp 309-316.

Small scale modelling

D.A. Olson, L.R. Glicksman, H.M. Ferm, August 1990, "Steady-state natural convection empty and partitioned enclosures at high Rayleigh numbers", Transactions of the ASME, Journal of Heat Transfer, Vol.112, pp.640-647

Flow visualization

Ren Anderson, Vahab Hassani, Allan Kirkpatrick, Kevin Knappmiller and Douglas Hittle, May 1991, "Visualizing the air flow from cold air ceiling jets", ASHRAE Journal, pp.30-35.

Appendix A Listing of code in Quick Basic, used for data acquisition to read temperatures

```
100 '*************************************************************************
110 '*          MODIFICATION OF
120 '*   EXAMPLE OF USING ONE EXP-16 WITH DAS-8 AND T THERMOCOUPLE *
130 '*          FOR TWO EXP-16s WITH DAS-16 AND T THERMOCOUPLES
140 '*************************************************************************

'---- STEP 1: Initialize an integer array D%(15) to receive data ------
 DIM D%(15)  '16 elements, one for each EXP-16 channel
 'Also initialize a corresponding real array to receive temperature data
 DIM TA(15)
 DIM TB(15)
 DIM TAA(15)
 DIM TBB(15)
 DIM ADdataA(15)
 DIM ADdataB(15)
 DIM AvA(15)
 DIM AvB(15)
 DIM X%(1000)
 DIM LT%(15)
 DIM CJ%(10)
 COMMON SHARED D%(), LT%(), X%(), CJ%()
 DECLARE SUB basdasg (mode%, BYVAL dummy%, flag%)
' DECLARE SUB CJC (CJC AS DOUBLE)
' DECLARE SUB Thermo (meas AS DOUBLE, channel AS INTEGER)


150 SCREEN 0, 0, 0: KEY OFF: CLS : WIDTH 80
160 'This example performs scanning and measurement of T type thermocouples
170 'connected to one EXP-16. The program can be expanded to handle multiple
180 'EXP-16's.
190 'Steps are:-
200 '       1 - Dimension other arrays and provide set up information
210 '       2 - Initialize DAS-8 and load thermocouple look up tables
220 '       3 - Measure temperature of connector block from CJC channel
230 '           (CJC = cold junction compensation)
240 '       4 - Measure output voltages of thermocouples on EXP-16
250 '       5 - Convert, correct and linearize thermocouple outputs to degrees
260 '       6 - Display output
270 'Note that thermocouple routines J.BAS, K.BAS etc. are in ASCII form and
280 'can be MERGE'd with any program and edited in.
290 '
300 'For purposes of example the EXP-16 output channel should be connected to
310 'DAS-8 channel #0 and the CJC channel to DAS-8 channel #7.

330 '---- STEP 2:  initialize -----
```

```
340 '
350 '
360 LOCATE 25, 1: COLOR 0, 7: PRINT "-PLEASE WAIT-"; : COLOR 7, 0: PRINT "
Loading DAS-8 I/O address and thermocouple lookup table data": LOCATE 1, 1
370 D%(0) = &H300 'initialize & declare CALL parameters

380 flag% = 0
390 mode% = 0            'Mode 0 = initialization
400 D%(1) = 2
402 D%(2) = 3
404 DASG = 0
406 CALL basdasg(mode%, VARPTR(D%(0)), flag%)
410 IF flag% <> 0 THEN PRINT "INSTALLATION ERROR"
420 '
430 'Load thermocouple linearizing look up data
440 GOSUB 50000
450 AV = 200 'Set gain setting of both EXP-16 boards

500 '----- STEP 2 1/2: Take average values for each channel and the CJC ----------
505 ' Initialize counters ADdataA, ADdataB and Cmeas
510 FOR I = 0 TO 15
520 ADdataA(I) = 0
530 ADdataB(I) = 0
540 NEXT I
550 Cmeas = 0

560 '-----------Averaging A, B and CJC readings ------------
570 'Add 3 consecutive readings
580 FOR J = 1 TO 3

600 '----- STEP 3: Get cold junction compensation temperature -------------
610 'Output of CJC channel is scaled at 24.4mV/deg.C. This corresponds to
620 '0.1 deg.C./bit. Dividing output in bits by 10 yields degrees C.
640 'Lock DAS-8 to channel #7 (CJC channel selected) using mode 1

650 mode% = 1: D%(0) = 7: D%(1) = 7
660 CALL basdasg(mode%, VARPTR(D%(0)), flag%)
670 IF flag% <> 0 THEN PRINT "ERROR IN SETTING CJC CHANNEL": END

704 D%(0) = 1              'number of conversions required
705 D%(1) = VARPTR(CJ%(0))   'provide array location
706 D%(2) = 1              'trigger source, 1=timer, 0=external on IP0
707 mode% = 4                'mode 4 - A/D to array
708 'Note 1: If the timer is used as a trigger source then holding input IP0
709 '       low will delay starting conversions.
710 CALL basdasg(mode%, VARPTR(D%(0)), flag%)
711 IF flag% <> 0 THEN PRINT "Error #"; flag%; " in mode 4": STOP
713 Cjc = CJ%(0) / 5
```

```
'714 PRINT CJC: END


740 '----- STEP 4: Get the thermocouple data -----------------------------
750 CH% = 0
760 GOSUB 21000
770 'This step is written as a subroutine so you can use it in your own
780 'programs by editing it out. Entry parameters are:-
790 '  CH% - specifies DAS-8 channel that EXP-16 is connected to (0-7).
800 '  D%(15) - integer data array to receive data from channels.

820 '----- STEP 5: Convert data to volts and linearize -------------------
830 'AV = Gain setting on Dipswitch of EXP-16 (change to suit).
840 FOR I = 0 TO 15
850 V = (X%(I) * 10) / (AV * 2048)
860 GOSUB 51000  'perform look-up linearization
870 TA(I) = TC       '= TF for degrees Fahrenheit
875 TAA(I) = (TA(I) - 16) * 3 / 8.16 + 16
880 NEXT I

1740 '----- STEP 4: Get the thermocouple data -----------------------------
1750 CH% = 1
1760 GOSUB 21000
1770 'This step is written as a subroutine so you can use it in your own
1780 'programs by editing it out. Entry parameters are:-
1790 '  CH% - specifies DAS-8 channel that EXP-16 is connected to (0-7).
1800 '  D%(15) - integer data array to receive data from channels.

1820 '----- STEP 5: Convert data to volts and linearize -------------------
1830 'AV = Gain setting on Dipswitch of EXP-16 (change to suit).
1840 FOR I = 0 TO 15
1850 V = (X%(I) * 10) / (AV * 2048)
1860 GOSUB 51000  'perform look-up linearization
1870 TB(I) = TC       '= TF for degrees Fahrenheit
1875 TBB(I) = (TB(I) - 16) * 3 / 8.16 + 16
1880 NEXT I

'     ----------Averaging loop ----------
'2065 GOSUB 3600 'Read CJC and temperatures from boards A and B

2070 Cmeas = Cmeas + Cjc
2080 FOR P = 0 TO 15
2090 ADdataA(P) = ADdataA(P) + TA(P)
2095 ADdataB(P) = ADdataB(P) + TB(P)
2100 NEXT P
2120 NEXT J

2220 'Divide total by number of readings (J ends up at 4, so -1)
```

```
2230 FOR H = 0 TO 15
2240 AvA(H) = ADdataA(H) / (J - 1)'2250 AvB(H) = ADdataB(H) / (J - 1)
2260 CJCav = Cmeas / (J - 1)

2270 'Scale temperatures with reference at 16 degC
2280 TAS(H) = (AvA(H) - 16) * 3 / 8.16 + 16
2290 TBS(H) = (AvB(H) - 16) * 3 / 8.16 + 16
2300 NEXT H

2900 '----- STEP 6: Display temperature data ----------------------------
2910 LOCATE 1, 1
2915 PRINT "                          EXP 0   EXP 1   Scaled temps."
2920 FOR I = 0 TO 15
2930 PRINT USING "Channel ## temperatures = ####.#, ####.#, ####.#, ####.# deg. C."; I;
TA(I); TB(I); TAA(I); TBB(I)
'1935 PRINT USING "Scaled temperatures     = ####.#,      ####.# deg. C."; TAA(I); TBB(I)
2940 NEXT I
2942 PRINT
2944 PRINT USING "Cold junction temperature (CJC) = ###.# deg. C."; Cjc
2950 GOTO 600   'repeat scan of channels

21000 '---- Subroutine to convert EXP-16 channels to number of bits --------
21010 'First lock DAS-8 on the one channel that EXP-16 is connected to.

21011 mode% = 1: D%(0) = CH%: D%(1) = CH%
21012 CALL basdasg(MD%, VARPTR(D%(0)), flag%)
21013 IF flag% <> 0 THEN PRINT "ERROR IN SETTING CJC CHANNEL": END

21050 'Next select each EXP-16 channel in turn and convert it.
21060 'Digital outputs OP1-4 drive the EXP-16 sub-multiplexer address, so use
21070 'mode 14 to set up the sub-multiplexer channel.

21080 FOR MUX = 0 TO 15
21090 mode% = 13
21095 D%(0) = MUX
21100 CALL basdasg(mode%, VARPTR(D%(0)), flag%)      'address set
21110 IF flag% <> 0 THEN PRINT "ERROR IN EXP-16 CHANNEL NUMBER": END

21140 mode% = 3  'do 1 A/D conversion
21150 CALL basdasg(mode%, VARPTR(D%(0)), flag%)
21160 IF flag% <> 0 THEN PRINT "ERROR IN PERFORMING A/D CONVERSION"
21168 X%(MUX) = D%(0)
 '1169 PRINT D%(0)
21180 NEXT MUX
'1181 END
21190 'All done - return from subroutine

21200 RETURN
```